Feasibility of Heat Pipes for High Performance Components in Airborne Applications

Thermal Integration Challenges and Design Strategies

Master's thesis in Mobility Engineering

Theresa Calisir
Elin Karlsson

DEPARTMENT OF MECHANICS AND MARITIME SCIENCES
CHALMERS UNIVERSITY OF TECHNOLOGY
Gothenburg, Sweden 2026
www.chalmers.se

MASTER'S THESIS 2026

Feasibility of Heat Pipes for High Performance Components in Airborne Applications

Thermal Integration Challenges and Design Strategies

Theresa Calisir
Elin Karlsson

Department of Mechanics and Maritime Sciences
CHALMERS UNIVERSITY OF TECHNOLOGY
Gothenburg, Sweden 2026

List of Acronyms

Abbreviation	Definition
BSGW	Bilateral Arch-Shaped Sintered-Grooved Wicks
CAD	Computational Aided Design
CFD	Computational Fluid Dynamics
CHF	Critical Heat Flux
CHP	Conventional Heat Pipes
DCCLHP	Dual Compensation Chamber Loop Heat Pipes
LHP	Loop Heat Pipes
MGW	Mesh Grooved Wicks
PHP	Pulsating Heat Pipes
SSGW	Single Sintered Grooved Wicks
TC	Thermocouple
TIM	Thermal Interface Material
UTHP	Ultra thin heat pipes
VC	Vapor Chamber

Abstract

This thesis focused on evaluating passive two-phase heat transfer technologies for potential use in airborne applications. The work included a background study of different heat pipe technologies, wick structures, working fluids and materials to identify suitable concepts for airborne conditions. The concepts were then assessed and compared using a weighted decision matrix based on requirements and constraints. The concept evaluation indicated that wick structure had a major influence on overall heat pipe performance. Sintered wick structures were considered the most favorable due to their reliable performance under varying conditions. The study also highlighted the importance of fluid-material compatibility. Although experiments were only performed on commercially available heat pipes, experimental testing generally confirmed the theoretical expectations. This included that sintered wick structures achieved the best overall performance, particularly in gravity-opposed orientations and that heat pipes with larger cross-sectional diameter demonstrated lower thermal resistance. The results obtained from the experiment also confirmed that higher heat loads and orientation strongly influence thermal performance. Overall, the study showed that passive two-phase cooling systems are promising for airborne applications, but concept selection involves important trade-offs between thermal performance, manufacturability and structural robustness.

Keywords: Heat pipe, wick structure, envelope material, working fluid, vapor chamber, TIM, gravity, airborne.

Acknowledgements

We would like to express our sincere gratitude to everyone who has contributed to this thesis and supported us throughout the project.

First, we would like to thank our supervisor and examiner, Mats Andersson, who has guided us during both our bachelor's thesis and now our master's thesis. Your support, feedback and encouragement throughout the years have meant a lot to us.

We would also like to thank Saab Huskvarna for giving us the opportunity to carry out this thesis project. A special thanks to our supervisors at Saab, Therese Nilsson and Annika Holmberg, for your support, guidance and involvement throughout the project.

We would like to thank Jonas Arwidson for generously sharing his expertise and for always showing great enthusiasm and interest in our work.

We also want to thank Beyond Gravity in Gothenburg for welcoming us for a study visit at their facility. The visit gave us valuable insight into the established heat pipe industry and provided a broader understanding of thermal management solutions in aerospace applications.

Finally, we would like to thank everyone else at Saab who has been involved in the project and contributed during the thesis work.

Table of contents

1. Introduction

Modern airborne systems rely more and more on high-performance electronics for communication, control and monitoring functions. As the performance demands increase, so does the amount of heat that is generated within these systems. Managing the heat is not only a design consideration but also a requirement to guarantee consistent performance and long-term reliability. Thermal management systems in airborne applications must withstand harsh environmental conditions, including vibrations, shocks and varying g-forces in multiple directions.

At the same time, there are a lot of strict constraints in avionics when it comes to keeping weight, size and energy consumption to a minimum. Traditional cooling methods, like forced convection or pumped liquid cooling, are often complex and require continuous maintenance which complicates their integration in tightly packed systems. On the other hand, passive two-phase heat transfer devices, such as heat pipes, offer a much more effective way of transporting heat without the need for mechanical power. This makes them an excellent choice for compact and performance-critical avionic environments.

1.1 Purpose

The purpose of the master's thesis is to investigate the possibility of implementing a passive two-phase cooling system into airborne applications, requested by Saab. The thesis will evaluate different types of heat pipes, as well as suitable inner structures (wicks) and relevant working fluids. These components will be evaluated based on their ability to operate effectively under typical airborne conditions.

The goal is to compare available technologies and identify the most suitable concept within the thesis constraints. By doing a background study, applying elimination processes and performing physical experiments, the thesis will provide a technical foundation for future implementation decisions.

1.2 Delimitations

Due to the limited time available for this thesis, the following delimitations apply:

- The thesis only investigates passive two-phase heat transfer devices. Active cooling systems are not included.
- The work focuses on how these devices could be integrated into avionics units at a concept level. Full certification or aircraft redesign is not part of the study.
- A detailed cost analysis is not included.
- Long-term testing beyond the project period is not performed.
- The results are based on the specific operating conditions defined for this project and may not apply to all airborne systems.

1.3 Research Question

The study is based on the following main research question:
Is it possible to use a passive two-phase heat transfer device in airborne avionics systems under the given operating and environmental conditions?

To answer this, the following sub-questions are examined:

- Which type of passive two-phase heat transfer device is most suitable for compact airborne systems?
- How do different wick structures and working fluids affect performance in airborne conditions?
- Can a prototype show reliable thermal performance under realistic mechanical and environmental loads?

2. Background Study

This chapter reviews the fundamentals of heat pipe technology as well as current developments, including different configurations, such as conventional heat pipes (CHP), loop heat pipes (LHP), vapor chambers and pulsating heat pipes (PHP). Particular emphasis is placed on wick structures, as they play a critical role in capillary performance and overall heat transfer efficiency.

2.1 Thermal Management Challenges in Airborne Applications

The increasing use of high-performance electronics and electromechanical components in airborne systems has made thermal management a key design consideration. Modern aircraft use advanced avionics, power electronics, sensors and communication systems that produce a significant amount of heat in small and tightly constrained spaces. If the heat is not properly managed it can lead to reduced performance, speed up the wear of components or cause failures in safety-critical systems (Shukla, 2015).

A major challenge in airborne thermal management is that conventional cooling methods are often impractical. Limits on weight, space and power restrict the use of large heat sinks, active air cooling or pumped liquid cooling systems. This is why passive thermal solutions are strongly preferred due to their low mass, high reliability and zero power consumption, which makes them well suited for safety-critical applications with limited maintenance opportunities. As a result, there is a need for compact thermal designs that can transport heat efficiently over short distances while maintaining minimal temperature gradients (Shukla, 2015).

Environmental conditions further complicate the thermal design. Airborne systems experience a wide range of temperatures, from extremely low temperatures at high altitudes to much higher temperatures inside tightly packed equipment bays. Furthermore, operating phases such as take-off, climb, maneuvering and landing cause thermal loads to change quickly. Such conditions place strict demands on thermal solutions to ensure stable

component temperatures and avoid large thermal stresses. Recent heat pipe studies show that achieving near-uniform temperatures under such changing and uneven conditions is especially difficult in densely packed electronic systems (Caruana & Guilizzoni, 2025).
Another challenge is the mechanical loads that airborne systems are exposed to. Vibration, shock and sustained acceleration (G-forces) can reduce the performance of thermal interfaces and heat transfer paths. Orientation changes are especially important since heat transfer mechanisms that depend on gravity or capillary effect perform differently when acceleration directions change. Consequently, airborne thermal solutions must tolerate frequent changes in orientation while still providing effective heat transfer and maintaining robust thermal contact between heat sources and cooling elements (Caruana & Guilizzoni, 2025).

Lastly, integration constraints also play a key role in airborne thermal management. Components are often packed tightly together, design tolerances are strict and reliability requirements are high, which leaves little room for design flexibility. As a result, thermal solutions usually need to be integrated directly into structural or electronic assemblies with minimal thermal resistance. Overall, thermal, mechanical, environmental and integration challenges make airborne thermal management especially demanding, motivating the use of advanced passive heat transfer solutions examined in this thesis.

2.2 Heat Pipe Technology

One solution to the thermal management challenges is the use of heat pipes. Heat pipes are passive two-phase heat transfer devices that transport heat from a heat source to a heat sink by utilizing the evaporation and condensation of a working fluid within a sealed enclosure. Heat is absorbed at the evaporator through phase change, transported by vapor flow and released at the condenser, while capillary forces return the liquid to the heat source, enabling efficient heat transfer with minimal temperature gradients. Thanks to their high thermal performance, passive operation and reliability, heat pipes are widely used in electronic cooling and aerospace applications (Ku, 2015). Heat pipes are sometimes bent because the system geometry requires it, in many applications the heat source and heat sink are not aligned, and the heat pipe must route heat through constrained spaces. Bending generally degrades heat pipe performance by increasing flow resistance inside the pipe. As the bending angle increases, the curvature of the vapor flow path creates additional hydraulic losses that hinder vapor transport from the evaporator to the condenser, resulting in higher evaporator temperatures and increased thermal resistance (Chang et al., 2025). An illustration of a heat pipe and its main components can be seen in Figure 1.

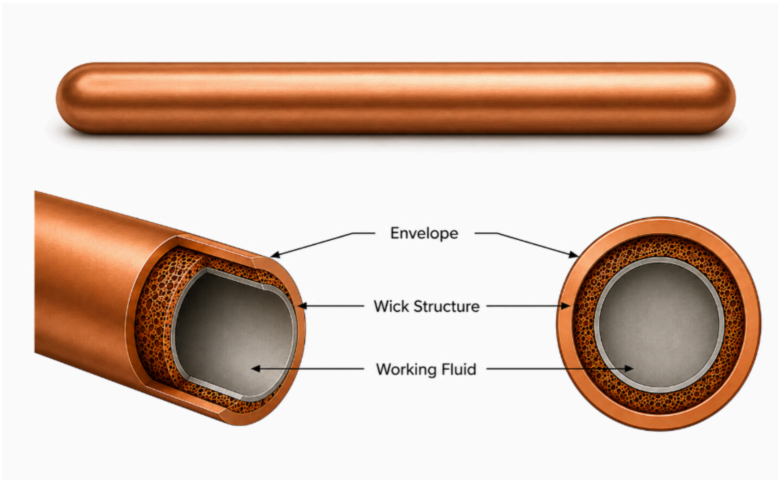

Figure 1: Schematic illustration of a heat pipe. AI-generated image created by the author using OpenAI, adapted from ACT (n.d.).

2.2.1 Heat Pipe Orientation

When the evaporator of a heat pipe comes in contact with an external heat source, heat is transferred into the liquid within the wicks of the evaporator. This causes the liquid to vaporize and moves to the condenser through the adiabatic region. At the condenser, the vapor condenses into liquid that moves to the evaporator through the wicks under capillary pressure (Shukla, 2015). The thermodynamic process is illustrated in Figure 2 and described below:

- Evaporator to adiabatic region (1→2): Heat supplied to the evaporator from external sources causes the working fluid to vaporize to either a saturated (2') or a superheated (2) vapor, undergoing an isothermal expansion.
- Adiabatic to condenser region (2→3): The vapor is driven by pressure through the adiabatic section toward the condenser, experiencing adiabatic expansion.
- Condenser to sink (3→4): The vapor condenses, releasing heat to the heat sink, undergoing isothermal compression.
- Condenser wick to evaporator wick (4→1): Capillary pressure generated by the menisci in the wick pumps the condensed fluid back into the evaporator, undergoing adiabatic compression.
- The process repeats.

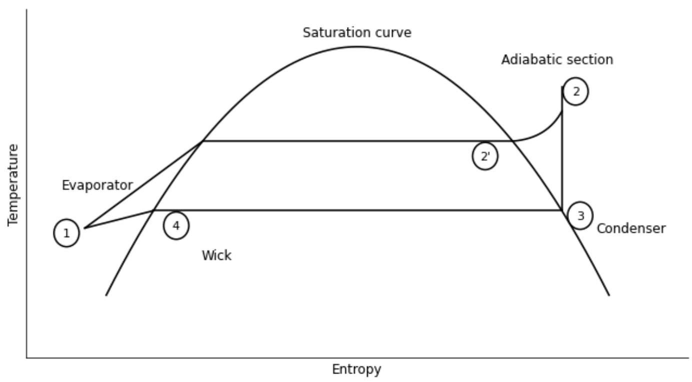

Figure 2: Heat pipe working principle.

2.2.2 Conventional heat pipes (CHP)

Conventional heat pipes (CHPs) are the most established and widely used type of heat pipe and are often used as the reference design for other heat pipe designs. A CHP is a sealed tube, typically manufactured from metals such as copper or aluminum, that is partly filled with a working fluid and internally lined with a porous wick structure. As shown in Figure 3, the heat pipe has three main sections: the evaporator, the adiabatic section, and the condenser. When heat is supplied at the evaporator, the working fluid absorbs the heat and vaporizes and flows toward the condenser due to the pressure difference. In the condenser, the vapor releases heat and condenses back into liquid. The wick structure uses capillary action to return the liquid to the evaporator, allowing continuous and passive heat transfer (Shukla, 2015).

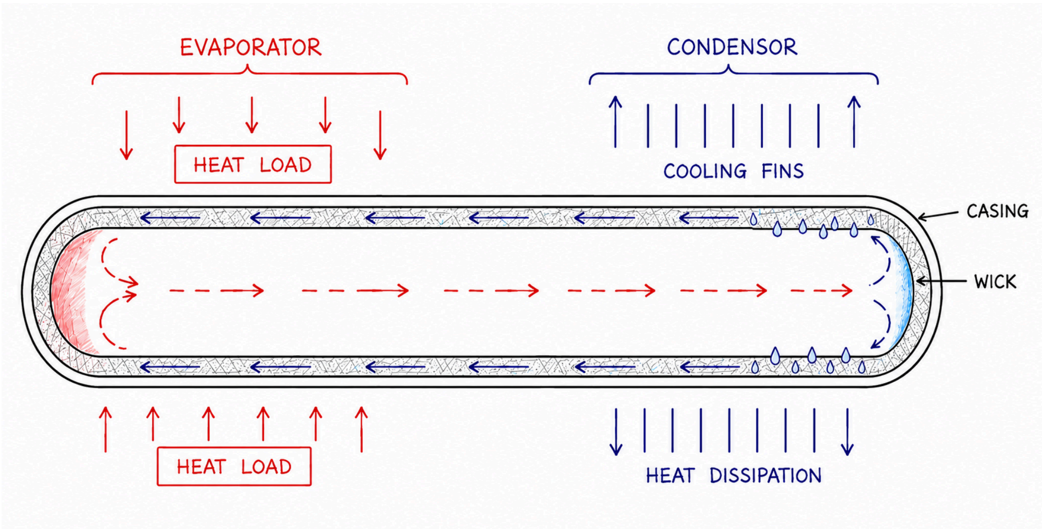

Figure 3: Principle of conventional heat pipe operation. AI-generated image created by the author using OpenAI, adapted from DNP (n.d.).

The wick structure is a critical component as it controls the capillary pumping ability and therefore the maximum amount of heat that can be transferred (McClements, 2023). Common wick designs include grooved wicks, screen mesh wicks and sintered wicks. Each type has different advantages and disadvantages in terms of capillary pressure and permeability. The choice of wick structure, working fluid and envelope material strongly affects the operating temperature range, thermal performance and reliability of the heat pipe. It is furthermore essential to emphasize that the working fluid and container material are chemically compatible for a stable and long-term operation.

CHPs are widely used in electronic cooling and aerospace systems due to their high effective heat transfer capability, low mass and passive operation. They are especially good for transporting heat away from localized hot spots to remote heat sinks while keeping temperature differences low. However, their performance is limited by several operating limits, including the capillary, boiling and sonic limits. As well as, the orientation of the heat

pipe and the presence of acceleration forces can affect the return of the working fluid and overall performance, which needs to be considered for integration of CHPs (Shukla, 2015).
In compact electronic systems, CHPs may need to be flattened to fit better in narrow spaces or make better contact with the surface of the hotspot. Flattening implies that the internal structure changes, which limits the space for the vapor to flow. This decreases the heat transport capacity. For airborne systems, mechanical stresses must also be considered. A flattened heat pipe (flat heat pipe) is more sensitive to vibration, acceleration and pressure differences at high altitudes. Repeated mechanical loading can deform the pipe walls over time. For these reasons, the amount of flattening must be carefully chosen to balance the integration and maintaining reliable heat transport (Wakefield Thermal, n.d.)

2.2.3 Vapor chambers (VC)

Vapor chambers are planar heat pipes that are used to spread heat across a surface instead of transporting it over a distance. Although their shape is different compared to CHPs, they work in the same way. When heat is applied to a specific area on the chamber, the working fluid absorbs it and evaporates. The vapor then moves within the pipe and carries the heat away from the hot spot. When it reaches the cooler region, it condenses and releases the heat over a larger area. Capillary forces return the condensed fluid through the internal wick structure, allowing the process to continue passively.
Vapor chambers are suitable in electronic and aerospace systems where available space for thermal management is limited. They are applied directly to the heat-generating component which allows the heat to be spread laterally before being rejected to a heat sink. This makes them especially useful for compact electronic devices that have hot spots. Their flat geometry makes them easy to integrate while their low mass and passive operation make them reliable for airborne conditions (Fu & Sundén, 2017). The operation of vapor chambers can be visually seen in Figure 4.

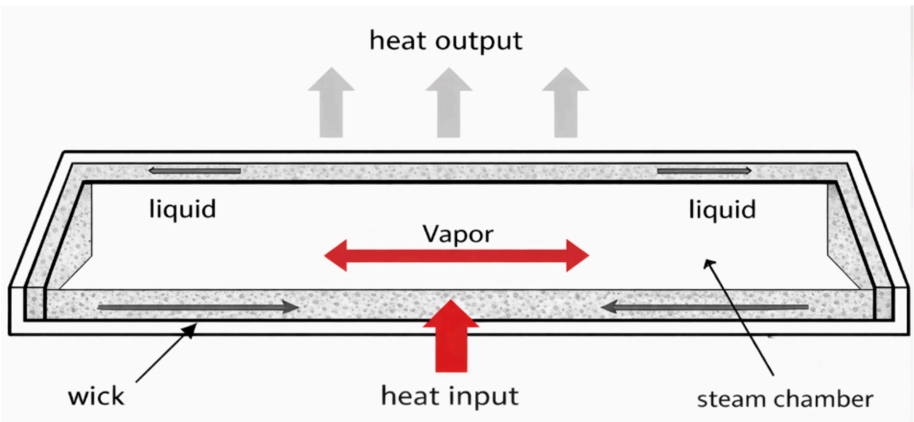

Figure 4: Principle of vapor chamber operations. AI-generated image created by the author using OpenAI, adapted from Han et al. (2020).

2.2.4 Loop heat pipes (LHP)

A loop heat pipe (LHP) is an efficient two-phase heat transfer device that moves heat from a source to a sink, using the evaporation and condensation of the working fluid. In contrast to simple heat pipes, LHPs are designed as a closed loop, in which liquid and vapor flow in separate paths, with circulation maintained by capillary action in a porous wick. The separated paths reduce the counterflow interaction and pressure losses, which allows the LHPs to transport significant amounts of heat over relatively long distances and in different orientations, including against gravity (Wang & Faghri, 2017).

At the core of a LHP is an evaporator containing a finely porous wick structure. When heat enters the evaporator from the heat source, the working fluid within the wick absorbs the thermal energy and evaporates, generating vapor and a pressure difference. The vapor produced at the evaporator is transported through a dedicated vapor line to the condenser, where it releases its latent heat to its surrounding cooler environment and condenses back into liquid. Separating the vapor and liquid flow paths reduces flow interaction and results in improved heat transfer performance (Wang & Faghri, 2017).

Once condensed, the liquid travels back through a liquid return line to a compensation chamber (reservoir) that is thermally linked to the evaporator. This chamber helps regulate the amount of liquid in the system and ensures stable operating pressure and temperature. Capillary forces in the wick draw the liquid back into the evaporator, from the chamber, to complete the cycle. Since this circulation is driven by capillary pressure generated from the small pores of the wick, no external pump is required as the fluid circulated passively as long as heat is supplied (Wang & Faghri, 2017).

LHPs combine the efficiency of CHPs, such as efficient latent heat transfer and low thermal resistance with additional improvements that allow them to operate under more demanding conditions. They can transport heat over long distances with minimal temperature losses and remain largely unaffected by gravity or orientation. Their flexibility and high heat transport capability make them useful in fields such as aerospace thermal control and high-power electronic systems (Wang & Faghri, 2017). The principle of LHPs can be seen in Figure 5.

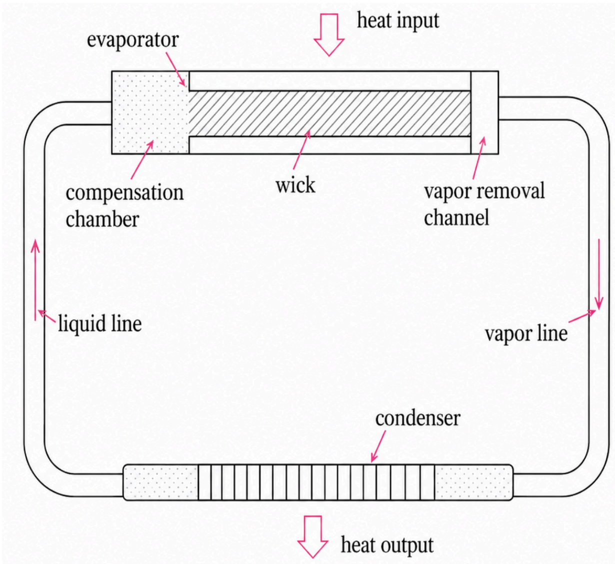

Figure 5: Principle of LHP operation. AI-generated image created by the author using OpenAI, adapted from Wang & Faghri (2017).

2.2.5 Pulsating Heat Pipe (PHP)

Pulsating heat pipes (PHP), also known as oscillating heat pipes, consist of a very thin, long and sealed tube that forms a serpentine or looped shape and is partially filled with a working fluid (Reay & Kew, 2007). Since the tube has such a small diameter, the fluid naturally separates into alternating liquid slugs and vapor bubbles. When heat is added to the evaporator, the vapor bubbles expand as the fluid evaporates. This causes the liquid slugs to push toward the other end of the tube - the condenser. Here, the pressure drops due to the condensation of vapor bubbles, returning them to liquid. This process of expansion and condensation of vapor bubbles causes the liquid-vapor mixture to move back and forth, see Figure 6. Heat is transferred both by the phase change of the working fluid and by the movement of the liquid slugs (Reay & Kew, 2007).

PHPs can be built in both open-loop and closed-loop. The closed-loop configuration is more commonly used because it provides a more stable oscillating motion and has better heat transfer performance. The PHPs performance depends on several factors like the working fluid, tube diameter, tube length, number of turns, filling ratio and orientation to gravity. Stable operation has been experimentally studied to be optimal when the filling ratio is between 25% and 65%. Outside this range, the back and forth motion can weaken or the evaporator may dry out (Reay & Kew, 2007). Since the working fluid is driven by pressure oscillations instead of by wicks with capillary action, PHPs may not be reliable under changing orientations.

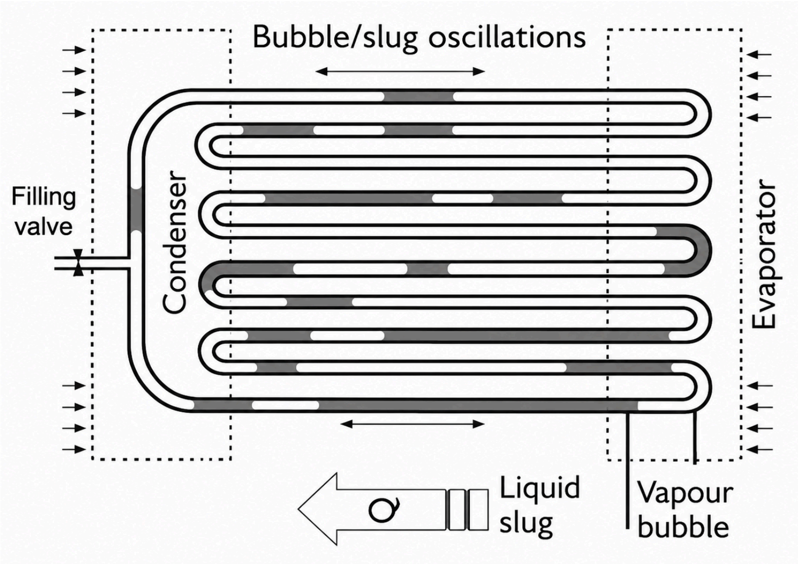

Figure 6: Operation of pulsating heat pipes. AI-generated image created by the author using OpenAI, adapted from Reay & Kew (2007).

2.2.6 Wick structures

Wick structures can be divided into two main categories: single structures and composite structures. Single wicks consist of more common designs, such as grooved, mesh and sintered wicks, while the composite wicks are formed by combining two or more of the single wicks. The geometry of the wick's channels or pores control both flow resistance and capillary pressure. However, there is a trade-off in the geometry where small pores generate stronger capillary pressure but reduce permeability, while larger pores allow easier liquid flow but provide weaker pumping force. Other properties such as how well the wick wets, how liquid spreads and where bubbles form during boiling are influenced by the surface roughness. The heat conduction through the wick and the available area for liquid flow are affected by the thickness of the wick (Caruana & Guilizzoni, 2025).

The wick provides the liquid flow paths needed to return the working fluid from the condenser to the evaporator and creates the pore structure required for capillary action. The wick is characterized by its permeability and effective pore radius. Together with the wick cross-sectional area, these parameters determine the wick's ability to overcome hydrodynamic pressure losses within the heat pipe (NASA, 1981).

Selecting an appropriate wick design requires balancing several competing factors. A small pore radius is needed to generate high capillary pressure, while high liquid flow rates require high permeability, which is generally associated with larger pore sizes. In addition, since the wick often lies directly in the heat transfer path, its thermal conductivity is also an important design consideration (NASA, 1981).
The different types of wick structures are visually illustrated in Figure 7.

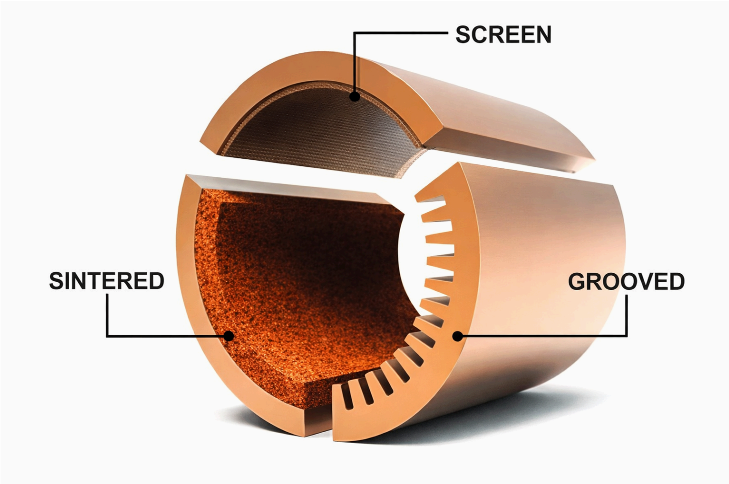

Figure 7: Visual illustration of different wick types. AI-generated image created by the author using OpenAI, adapted from Momin (2020).

2.2.6.1 Grooved wicks

Grooved wicks are widely used because of their high permeability, manufacturability and low cost, at the expense of low capillary pressure. Groove channels can be produced in different geometries, U-shaped and V-shaped grooves being the most common. Channel width and height influence permeability and the curvature of the liquid-vapor interface, while the channel length controls the dryout length (Egbo et al., 2026). Because of their fast thermal response, high permeability, lightweight design and structural stability, grooved wicks are favored in electronics. They are also used in cylindrical heat pipes, flat heat pipes and vapor chambers. Grooved wick structures can be produced using a range of fabrication methods. Traditional machining techniques, such as milling or high-speed spinning, allow efficient production of flat and cylindrical heat pipes, but they could be limited in groove proportions and surface finish. Other machining methods, including laser processing or electrical discharge machining, allow more precise and complex geometries and often incorporating features to enhance capillary performance. Methods such as additive manufacturing also enable more complex and high-performance wicks with enhanced capillary pressure and permeability, however it also brings increased costs and complexity (Tang et al., 2024).

2.2.6.2 Sintered wicks

A sintered wick, also referred to as a powder-sintered wick, is a porous structure formed by bonding metal powders through a sintering process to create an interconnected network of pores. This structure generates strong capillary forces, allowing efficient transfer of the working fluid from the condenser back to the evaporator, even under anti-gravity conditions and over extended flow lengths. Due to the high capillary pressure and orientation-independent performance, sintered wicks are widely used in heat pipes for high flux applications. The permeability and capillary behavior are mainly influenced by porosity, powder particle size and pore connectivity, which can be tailored through material selection and processing control. Compared to grooved wicks, sintered wicks have much higher capillary force but generally lower permeability. Compared to composite wicks, sintered wicks have a simpler structural integration and a more uniform distribution of the fluid. The most common powders used are copper and stainless steel, because of their sintering behavior, while aluminum powders are currently explored increasingly for their lightweight and cost-effective solutions. However, aluminum oxide hinders sintering, requiring advanced methods for high-performance heat pipes (Tian et al., 2025).

2.2.6.3 Screen mesh wicks

Screen mesh wicks are among the most commonly used wick structures in heat pipes due to their low cost, manufacturability and availability. They consist of one or more layers of woven metal mesh pressed against the inner wall of the heat pipe, creating a porous capillary network that facilitates liquid return from the condenser to the evaporator. An effective balance between capillary pressure and permeability is provided, leading to low thermal resistance at moderate heat inputs. However, increasing mesh fineness reduces permeability and can markedly restrict the maximum heat transport capacity. A key drawback of screen mesh wicks is their lack of structural attachment to the wall in the heat pipe, making them particularly vulnerable to deformation during bending. Such deformation may lead to buckling and partial detachment from the wall, disrupting the liquid return, increasing pressure drops at liquid-phase and triggering premature dryout. By aligning the mesh at a bias to the heat pipe axis, flexibility and resistance to bending are increased, helping the screen mesh wick heat pipes maintain a stable thermal performance under mechanical stress (Guinan et al., 2026).

2.2.6.4 Composite wicks

Composite wicks, which combine grooved structures with sintered powders or mesh layers, have been studied for enhancing thermal performance in both ultra thin heat pipes (UTHPs) and LHPs. In UTHPs, wick designs such as single and bilateral arch-shaped sintered-grooved wicks (SSGW and BSGW) and mesh grooved wicks (MGW) provide a balance between large vapor channels and reasonable capillary pathways, ensuring smooth fluid flow without risk of dryout. Typically these wicks are fabricated by sintering copper powder or mesh onto grooved structures, achieving radial uniformity, while porosity and groove volume are carefully characterized to optimize fluid and vapor distribution. Similarly, in LHPs, composite wicks are used to limit heat leakage from the evaporator to the compensation chamber (Li et al., 2016). Combining highly conductive sintered copper and ultra-low conductivity ceramic powder leads to the wicks facilitating rapid evaporation at the heating surface while thermally isolating the compensation chamber. LHPs with composite wicks offer lower startup temperatures, reduced operating temperatures under moderate heat loads and improved steady-state thermal performance compared to mono-material wicks. However, at high heat fluxes, interfacial resistance between wick materials can obstruct fluid replenishment, diminishing the thermal benefits of the composite structure (Xiong et al., 2024).

The key characteristics and performance trade-offs of the different wick structures are summarised in Table 1.

Table 1: Comparison of different wick types.

Wick type	Capillary pressure	Permeability	Orientation sensitivity	Manufacturing complexity	Notes
Grooved	Low	High	High	Low	Lightweight and low-cost; suitable when orientation is favorable. Limited capillary pumping under maneuvering conditions.
Sintered (powder)	High	Moderate–Low	Low	High	Strong capillary action and reliable under variable gravity and g-loads; higher mass and manufacturing complexity.
Screen mesh	Moderate	Moderate	Moderate–High	Low	Cost-effective and easy to fabricate; may deform under vibration or bending, risking dryout.
Composite	High	High	Low	Very high	Combines strong capillary pumping and good vapor flow; improved dryout resistance but complex fabrication and possible interface resistance.

2.2.7 Working fluids

The selection of a heat pipe working fluid depends primarily on the operating temperature and the compatibility with the material of the container. According to NASA (1981), working fluids are categorized by temperature range: cryogenic fluids such as hydrogen, helium or nitrogen for extremely low temperatures, low-temperature fluids, including alcohols and halocarbons, for temperatures below ~100 °C, moderate-temperature fluids, such as water, for ~100-300 °C and high-temperature fluids, typically liquid metals such as sodium, potassium or lithium, for temperatures above 500 °C. Material compatibility is essential to prevent corrosion or chemical reactions with the container or wick. Vapor pressure affects containment requirements, while viscosity and pore size affect capillary flow and overall heat transfer. Thermal properties, such as latent heat and thermal conductivity, determine heat pipe efficiency, and fluid purity is crucial to avoid clogging or reduced performance. These factors together guide the selection of an appropriate working fluid that ensures reliable and effective heat pipe operation (NASA, 1979).

When comparing different working fluids, mainly in terms of the thermophysical properties and the influence it has on pressure drop, liquid-vapor interface shape, critical heat flux (CHF) and total thermal resistance (R_{tot}) in a micro-grooved heat pipe. Water, methanol, acetone, pentane and ammonia were the fluids analyzed, where water stood out as the most favorable due to having the lowest pressure drop along the pipe and a more gentle curvature of the liquid-vapor interface, where both are associated with stronger capillary performance and a higher CHF. As a result, water typically showed lower thermal resistance, especially at low to moderate heat inputs. Pentane shows the weakest behavior, with the largest pressure drop and strong interface curvature, indicating poor capillary performance and a low capillary limit. This makes it less effective, especially at higher heat inputs. Methanol and acetone lie in between but can be competitive depending on heat load and operating conditions. Ammonia contrasts with water, as heat input nears ammonia's capillary limit, their thermal resistance converges, indicating that fluid choice depends on the operating heat load (Arab & Abbas, 2014).

Water is typically the most commonly used working fluid, especially in combination with copper for electronics cooling and moderate-temperature applications. Ammonia is frequently used in spacecraft thermal control and LHPs, as it performs well at low to moderate temperatures and remains reliable under space conditions. Alcohols, mainly methanol and ethanol, are also commonly used in aerospace and micro heat pipe applications because of their suitable operating temperature ranges. Acetone is used in cryogenic heat pipes and vapor chambers, where relatively low operating temperatures and planar geometries are involved. Refrigerants such as Freon-11, Freon-21 and Freon-113 have been particularly used in aerospace and electronics cooling applications. As they are compatible with aluminum heat pipes, they are attractive to lightweight aerospace structures. They have relatively low boiling points and their favorable vapor pressures allow operation at low to moderate temperature. However, the use of many Freons has declined due to their ozone depletion potential and high global warming impact, resulting in an increase in replacing them with more environmentally friendly alternatives. For high-temperature applications, especially in hypersonic vehicles and advanced aerospace systems, liquid metals such as sodium and lithium are preferred because of their thermal stability at elevated temperatures (Shukla, 2015). Material compatibility is a strict constraint when selecting a working fluid. Incompatible combinations can lead to corrosion, chemical reactions, formation of galvanic cells or decomposition of the working fluid at elevated temperatures. These effects can degrade thermal performance and also cause structural failure of the heat pipe (Shukla, 2015).
A water-charged heat pipe can transfer the same heat as R134a with a smaller temperature drop. Water also operates at lower internal pressures than refrigerants at the same temperature, which can allow thinner pipe walls and reduced system weight (Jouhara & Meskimmon, 2018). However, R134a is compatible with common engineering metals used for heat pipe fabrication, such as stainless steel, nickel, copper and aluminum and has a much lower freezing point than water (Wang et al., 2020). Working fluids, along with their boiling points, critical temperatures and compatible materials are shown in Table 2.

Table 2: Characteristics of working fluids.

Working Fluid	**Melting Point (°C)**	**Critical Point (°C)**	**Compatible Material**
Methanol	-97	240	Stainless Steel, Iron, Copper, Brass, Silica, Nickel
Ammonia	-78	132	Aluminum, Stainless Steel, Iron, Nickel, Cold Rolled Steel
Toluene	-95	321	Stainless Steel, Copper, Nickel, Carbon Steel
Acetone	-95	235	Aluminum, Stainless Steel, Copper, Brass, Silica
n-Heptane	-91	267	Aluminum
Freon-11	-111	198	Aluminum
Freon-21	-135	179	Aluminum, Iron
Water	0	373.95	Copper, Stainless Steel, Nickel, Titanium
R134a	-101.1	100.9	Stainless Steel, Nickel, Copper, Aluminum

2.2.8 Materials

The materials most commonly used for heat pipes are copper, aluminum alloys, stainless steel and nickel-based alloys for high-temperature applications. Material selection is mainly determined by factors such as thermal conductivity, structural strength, resistance to corrosion, manufacturability and chemical compatibility with the chosen working fluid (NASA, 1981).

Aluminum offers several important characteristics that make it suitable, particularly for aerospace and lightweight systems. Aluminum heat pipes are characterized by lightweight construction due to having low density. Along with structural stability and strong performance when properly optimized. Aluminum as an envelope material provides moderate intrinsic thermal conductivity which enables effective heat spreading. In aluminum-acetone heat pipes specifically, its performance is influenced by the properties of acetone. The low surface tension reduces capillary pressure in the wick, limiting liquid return against gravity, and its lower latent heat of vaporization requires higher mass flow rates for a given heat load. As a result, aluminum heat pipes perform best with gravity assistance and need optimized wick design and filling ratio to avoid dry-out (Liang et al., 2026).

Copper is another material commonly used in heat pipes since it combines high thermal conductivity with exceptional capillary and manufacturing properties. Its high thermal conductivity allows rapid heating from the evaporator, reducing hot spots and improving temperature uniformity. In porous form, copper provides a large internal surface area that facilitates effective evaporation and stable boiling. Its surface properties can be adjusted to enhance wettability, improving liquid distribution and capillary pumping capability. Furthermore, copper is also mechanically robust and easy to fabricate and seal, making it well suited for compact heat pipes operating under high heat flux conditions (Wang et al., 2025).

Stainless steel is used because of its high mechanical strength, corrosion resistance and high-temperature stability, making it suitable for harsh operating environments. However, the performance of stainless steel heat pipes depends more on wick structure than the metal envelope. The main trade-off is that the traditional stainless steel wire mesh wicks provide high permeability but low capillary pressure, while sintered powder wicks offer higher capillary pressure but lower permeability. To overcome this trade-off, composite wicks can be used to improve overall thermal performance, however this will bring an increase in cost and manufacturing complexity (Huang et al., 2019).

Nickel is used for its balanced thermal, chemical and mechanical properties, especially in demanding environments. Even though the thermal conductivity for nickel is lower than copper, it is sufficient for moderate to high-temperature applications, especially where corrosion resistance and strength are important. Nickel offers excellent corrosion resistance due to its stable oxide layer, ensuring compatibility with different working fluids and long-term reliability. It maintains mechanical strength at high temperatures, has a high melting point and withstands stress and thermal cycling. Overall, nickel is valued for its durability, chemical stability and strong performance at elevated temperatures rather than maximum heat transfer efficiency (Hansen & Næss, 2015).

Titanium is mainly chosen for its high strength-to-weight ratio, providing a lightweight yet robust heat pipe that can tolerate high internal vapor pressure at elevated temperatures. Titanium also offers strong corrosion resistance and minimal thermal expansion, contributing to improved structural integrity and reliable performance during continuous temperature fluctuations. Even though titanium's intrinsic thermal conductivity is lower than copper's, heat pipe performance is dominated by phase-change heat transfer and wick-driven liquid return, so the bulk conductivity of the bulk material matters less. Titanium is mostly used in aerospace-related fields due to its lightweight construction, corrosion resistance and mechanically strong properties. However it is a material very high in cost and manufacturing complexity (Wang et al., 2025).

2.3 Heat Pipes in Airborne Conditions

Heat pipes used in airborne applications are exposed to conditions that are completely different from what stationary electronic systems encounter. Changes in orientation, acceleration, vibration, pressure and temperature can have great influences on the heat pipes and therefore influence the thermal performance and reliability. This section reviews how such airborne conditions affect heat pipes in general and highlights how each type differs from each other.

2.3.1 Orientation and Gravity

Conventional and flat heat pipes are both wick-based and therefore affected by their relative position of the evaporator and condenser. Thermal performance is generally better when gravity can assist the flow compared to anti-gravity operation which increases the load on the capillary structure (Qats, 2013). Flat heat pipes benefit from their planar geometry which makes them less sensitive to orientation compared to round heat pipes. However, this does not make them fully independent of gravity and may still work less effectively if oriented in unfavorable positions for a long time.

LHPs are also wick-based and are specifically designed to withstand changes in orientation. They are built in a way that allows high capillary pressures to be generated in the evaporator which keeps the return of the fluid to condenser stable, even during anti-gravity operation. This is why LHPs are regarded as the superior type when it comes to orientation-tolerant passive two-phase devices. This makes them especially suitable for aerospace applications where the operating orientation cannot always be controlled (Guo et al., 2020).

Pulsating heat pipes are not wick-based and instead rely on a back and forth motion to push the working fluid. The motion is driven by pressure oscillations rather than capillary pumping, which makes their thermal performance strongly dependent on orientation. Changes in gravity direction can disturb the oscillation patterns and cause unstable or reduced heat transfer. This makes PHPs limited in applications with rapidly varying orientation.

2.3.2 Acceleration and G-forces

Airborne environments also expose the heat pipes to varying acceleration levels caused by maneuvers, turbulence and general operational loads. Acceleration acts like an additional gravity force on the working fluid. Depending on the direction of the acceleration, it can either help the flow or make it more difficult. In wick-based heat pipes, acceleration in the opposite direction of the flow increases the capillary pressure that is necessary to keep the circulation going which reduces its heat transport capability.

LHPs are generally more tolerant to acceleration effects. They can create high capillary pressure in the evaporator wick. Their design separates the liquid and the vapor flows which helps them continue working reliably. PHPs react more strongly to sustained acceleration since it may disturb the oscillations.

2.3.3 Vibration

Vibration is an important consideration for aircraft LHP applications since the system is exposed to continuously varying accelerations caused by high speed airflow and machinery onboards. Previous work has mainly focused on constant acceleration rather than periodically varying acceleration (i.e., vibration), and its effects are therefore less well understood.

A study performed by Wang (Wang, et al., 2025) showed that the effects of vibration on a dual compensation chamber LHP (DCCLHP) performance depend mainly on the operating heat load. At high heat loads (800-1000W) vibration had a negligible influence, with temperature variations on the order of only 1°C. This effect was attributed to the evaporator core and compensation chambers being nearly fully liquid-filled. Under constant-conductance state, structural confinement limits liquid motion, reducing the vibration-induced changes in liquid distribution and heat leak.

At low heat loads (200W), the DCCLHP becomes more sensitive to vibration because a larger free liquid-vapor interface allows easier liquid redistribution. Low frequency vibrations were observed to raise the vapor temperature, especially when the vibration was aligned with the evaporator axis, with a maximum increase of 8,8°C reported at 5 Hz. This was attributed to vibration-induced sloshing that reduced liquid in the evaporator core, leading to greater heat leak and higher operating temperature.

As vibration frequency increased, amplitude decreased and the liquid distribution approached the static case. High frequency vibration could slightly reduce vapor temperature by enhancing internal heat transfer and cooling of the returning liquid. Peak acceleration showed a non-monotonic and not statistically significant, with temperature deviations typically below 3,5°C. Additionally, temperature oscillations were observed under a low-frequency vibration at low heat loads, especially when the vibration direction was parallel to the evaporator axis, consistent with cyclic variations in heat leak driven by fluctuating liquid distribution (Wang et al., 2025).

PHP operation can be significantly affected by external vibrations, altering the internal two-phase flow dynamics. According to the reviewed literature, vibration can assist in detaching vapor bubbles from the channel walls and improve the transport and return of liquid droplets in the condenser section, enhancing circulation and heat transfer efficiency. Since the motion of the working fluid in a PHP can be described as a forced and damped oscillatory system, externally imposed vibrations can interact with the natural oscillation of the liquid plugs. When the externally imposed vibration frequency approaches the natural frequency of the plug-slug system, resonance-like behavior may arise, resulting in amplified oscillations and improved fluid circulation. Furthermore, the inertial effects associated with vibration can reshape the liquid plugs and modify the effective contact angle at the wall, thereby influencing capillary-driven transport and the overall stability of the two-phase flow within the system (Li et al., 2025).

CHPs and VCs are also affected by vibration, since the vibration can redistribute the working fluid and influence the liquid-vapor interface. However, the wick structure helps maintain liquid return to the evaporator, making them generally less sensitive to vibration compared to PHPs. VCs may be even less sensitive due to their planar geometry and more even liquid distribution.

2.3.4 Other Environmental Conditions

Heat pipes are also exposed to environmental conditions like changes in ambient pressure, corrosive surroundings and repeated temperature variations. Although heat pipes are sealed with the working fluid being the only factor affecting the internal pressure, the external pressure changes can create a pressure difference on the casing. This is especially a problem for thin or flattened designs which are most sensitive to mechanical stresses. This is why the casing material and the joining method must be strong enough to avoid deformation or leakage during operation (Fu & Sundén, 2017).

Operations in humid climates or coastal areas expose the device to salt spray. Salt particles can build up on the surface and slowly weaken the casing if it is not coated with corrosion-resistant materials. Chemical exposure can also occur from hydraulic fluids, cleaning agents, de-icing fluids or fuel vapors. These substances damage the protective coating and can react with certain materials. Therefore, there needs to be compatibility between the casing, the wick structure and the working fluid to avoid internal degradation over time (Fu & Sundén, 2017). Lastly, another factor to take into account in the mechanical design is repeated temperature changes that create thermal stresses due to the heat pipe and surrounding structures expanding differently.

2.4 Integration and Thermal Interfaces

Another challenge is how to mount the heat pipe in the surrounding structure. In compact electronic systems, the path from the heat source to the evaporator is very important and if the thermal resistance is too high, the benefit of the two-phase heat transfer can be reduced.

Heat transfer at the contact surface is limited by thermal contact resistance. In reality, no surface is completely smooth even if surfaces are carefully machined they still have small rough areas. When the heat pipe is pressed against the heat source, there still remains small air gaps. Since air conducts heat poorly, these gaps increase the thermal resistance and reduce heat transfer. The size of this resistance depends on the material, surface finish, contact pressure and whether thermal interface materials (TIMs) are used. Increasing the contact pressure improves the contact between the surfaces and reduces resistance. However, in aircraft systems the allowed pressure is limited because of structural and vibration requirements. TIMs such as thermal grease or gap fillers can help by filling the small gaps. At the same time, their thickness and long-term stability under vibration and temperature changes must be considered. If the layer is too thick, it increases thermal resistance and reduces cooling performance.

Mechanical integration must also consider limited space and operational loads. Avionics units are compact and exposed to vibration, acceleration and repeated temperature changes. Small differences in dimensions between parts can create gaps or uneven loading. This can deform thin heat pipe casings and affect the internal wick structure, especially in flat designs. Therefore, stable mounting methods are needed to maintain good contact during operation. If the heat pipe needs to be bent, the minimum bending radius must be followed to avoid damaging the internal structure and reducing its ability to transport heat.

3. Requirements and Constraints

The thesis follows a set of operational and environmental requirements provided by Saab. These requirements set the boundaries and act as constraints when comparing and selecting different concepts. The constraints are explained in the following paragraphs as well as summarized in the table below, see Table 3.

The heat pipe must operate within a temperature range at the heat source from −55 °C to +125 °C. This range represents extreme conditions that can occur during ground operation, high-altitude flight and different mission phases. The selected working fluid and envelope material must remain stable within this interval so that the fluid does not freeze or generate excessive vapor pressure.

The heat pipe must be integrated into a card module consisting of a PCB (Printed Circuit Board) and a metallic frame. The module is inserted into a mechanical chassis that provides the interface to multiple card modules. The combined thickness of the heat pipe and the TIM layer must not exceed 10 mm. The metallic frame of the card module has overall dimensions of 207 × 140 mm, which defines the available area for heat pipe integration. The heat pipe must therefore be integrated within this frame structure, preferably along either the long side or the short side of the frame. A shorter heat transport distance is generally preferable, as it reduces thermal resistance and improves overall heat transfer performance.

The solution must operate when the aircraft is oriented horizontally, vertically, and at a 45° angle. Since airborne systems change orientation during flight maneuvers, the thermal performance cannot rely solely on gravity-driven liquid return. The selected concept must therefore maintain adequate thermal performance under these orientations. In addition, the influence of acceleration and G-forces should be considered qualitatively.

Airborne environments also expose components to continuous vibration and occasional mechanical shocks. The selected concept must withstand these loads without structural failure, deformation of the wick structure or disruption of the internal fluid circulation.

Operation at altitudes from ground level up to 45,000 ft must also be considered. Even though a heat pipe is a sealed system and its internal pressure depends on the working fluid, changes in external pressure create mechanical stress in the envelope. The material strength and joining methods must therefore ensure structural integrity throughout the altitude range. Furthermore, exposure to salt spray and chemical fluids such as hydraulic oil, cleaning agents and fuel vapors must be taken into account. The casing material and any surface treatment must provide sufficient corrosion resistance. In addition, compatibility between the working fluid, wick structure and envelope material must be ensured to prevent long-term degradation.

Table 3: A summary of the operational and environmental constraints that define the design boundaries for the selected heat pipe concept.

Constraint	**Requirement/limit**
Temperature range	-55°C to +125°C
Maximum height	$\leq$ 10 mm
Orientation	Vertical, horizontal and 45°operation
Acceleration / G-forces	Airborne maneuvers
Vibration & Shock	Continous vibration + occasional shocks
Altitude	Ground level to 45,000 ft
Chemical exposure	Salt spray, hydraulic oils, cleaning agents, fuel vapors

4. Concept Development

To determine the most suitable heat pipe concept, each key component must be systematically evaluated and compared. The evaluation focused on the main design elements of a heat pipe: heat pipe type, working fluid, wick structure, and envelope material.

First, an elimination matrix was created for each category. In this step, all alternatives that did not meet the defined constraints were eliminated. This ensured that only solutions that satisfied basic requirements moved forward in the process. The remaining solutions from each matrix were then combined in a morphological matrix. The software Morpheus was used to generate all possible concept combinations while considering incompatibilities between different elements.

Lastly, the generated concepts were evaluated using a weighted decision matrix. Each concept was assessed based on predefined criteria and the concepts were ranked to identify the most suitable solution.

4.1 Elimination of Heat Pipe Type

The heat pipe elimination matrix was developed to evaluate the suitability of the different types of heat pipes, including LHPs, VCs, PHPs and CHPs against the specified mechanical and operational constraints, as seen in Table 4. The maximum thickness requirement (≤10 mm) is considered achievable for all configurations, except for LHP. Loop heat pipes consist of several components (evaporator, compensation chamber, vapor and liquid lines), which complicates integration in compact systems and imposes a strict thickness limit of 10 mm. Therefore, LHPs were excluded from further consideration.

Orientation independence and resistance to acceleration are mainly determined by capillary pumping strength and flow stability. LHPs are generally more robust under varying gravity and G-loads due to their separated liquid and strong capillary pumping. VCs and CHPs can also operate in different orientations when properly designed, while PHPs are more sensitive to gravity and acceleration due to their oscillating two-phase flow. All configurations can meet vibration and shock requirements when properly designed, as their operation is not directly influenced by these loads and can therefore be considered compliant.

Table 4: Elimination matrix for heat pipe type.

Constraint / Criterion	**LHP**	**Vapor Chamber**	**PHP**	**CHP**
Maximum thickness (≤ 10 mm)	×	✓	✓	✓
Orientation	✓	✓	×	✓
Acceleration / G-forces (Airborne maneuvers)	✓	✓	×	✓
Vibration & shock (Continuous vibration + occasional shocks)	✓	✓	✓	✓

4.2 Elimination of Working Fluids

Next is the elimination matrix for working fluids, see Table 5. Table 5 illustrates the elimination of working fluids based on their compliance with the required melting temperature (T_m), critical temperature (T_c) and environmental regulations.

Water has its freezing point above -55°C, which would prevent reliable operation at the minimum required temperature and was therefore eliminated. In many electronic cooling applications, the heat pipe begins operating once the system temperature rises above the freezing point, making frozen start-up a manageable design consideration. R134a was eliminated since its critical temperature is below 125°C, making it unsuitable for the specified maximum operating temperature. “Regulatory OK” refers to whether the working fluid complies with current environmental regulations. The refrigerants, such as Freon-11 and Freon-21, have been phased out due to their ozone depletion potential and environmental impact.

Table 5: Elimination matrix for working fluids

Working Fluid	$T_m < -55°\mathbf{C}$	$T_c > 125°\mathbf{C}$	**Regulatory OK**
Methanol	✓	✓	✓
Ammonia	✓	✓	✓
Toluene	✓	✓	✓
Acetone	✓	✓	✓
n-Heptane	✓	✓	✓
Freon-11	✓	✓	×
Freon-21	✓	✓	×
Water	×	✓	✓
R134a	✓	×	✓

Table 6 presents the updated fluid-envelope material compatibility matrix for the remaining working fluids and envelope materials. The matrix evaluates whether each fluid-material combination is chemically stable and suitable for long-term heat pipe operation. Compatibility is essential to prevent corrosion, chemical degradation or gas formation within the system, to keep a viable capillary performance and structural integrity. Titanium is generally chemically compatible with organic working fluids and can be considered a viable envelope material. However, due to manufacturing complexity, cost and lower thermal conductivity compared to Cu and Al, it is less commonly used in moderate-temperature heat pipes in avionics.

Prior to moving forward to the concept selection stage, two of the working fluids were eliminated. Firstly, n-Heptane was eliminated due to having a lower surface tension than alcohol-based working fluids, which reduces the capillary pressure that can be generated in a wick. According to capillary limit theory (NASA, 1981) and comparative studies for hydrocarbons (Arab & Abbas, 2014), fluids with low surface tension tend to have higher sensitivity to pressure losses and lower capillary limits, making them less suitable for acceleration sensitive heat pipe applications. Secondly, toluene was eliminated, even though it is thermally viable, due to its flammability and flow resistance (Reay & Kew, 2007). In addition, it has a higher liquid viscosity than the alcohol-based fluids, which increases pressure losses in the wick and reduces the available capillary margin. Of the remaining working fluids, only combinations marked as compatible were carried forward to the concept selection stage.

Table 6: Updated fluid-envelope material compatibility matrix

HP Material / Working fluid	Al	Cu	SS	Ni	Ti
Methanol	×	✓	✓	✓	✓
Ammonia	✓	×	✓	✓	✓
Toluene	×	✓	✓	✓	✓
Acetone	✓	✓	✓	×	✓
n-Heptane	✓	×	×	×	✓

4.3 Elimination of Wick Structures

To further narrow down the heat pipe configurations, an elimination matrix was developed to evaluate the suitability of different wick structures for the specified airborne application and can be seen in Table 7. The assessment considered orientation independence, heat flux capability, cold start performance at -55°C, and robustness under vibration and G-forces.

Since the heat pipe must operate in both vertical and horizontal orientations, adequate capillary pumping capability is required. Grooved wicks are eliminated due to their limited capillary pressure and dependence on gravity assisted liquid return. The heat flux criterion assesses the wick's ability to sustain high local heat input without reaching the capillary limit or causing dry-out. Grooved and screen mesh wicks provide limited capillary pressure, making them unsuitable for higher heat flux conditions. The cold start criterion evaluates the ability of the wick to redistribute liquid and initiate stable operation at low temperatures. All wick structures were considered capable of functioning at -55°C, assuming that the working fluid remains in a viable phase range. All wick structures were evaluated as mechanically robust and capable of maintaining stable operation under expected vibration and acceleration loads.

Table 7: Elimination matrix for wick structures.

Wick structure	Orientation	Heat flux	Cold start (-55°C)	Vibration/G-force
Grooved	×	✓	✓	✓
Sintered	✓	✓	✓	✓
Screen mesh	✓	×	✓	✓
Composite	✓	✓	✓	✓

4.4 Elimination of Envelope Material

Table 8 represents an elimination matrix to evaluate suitable envelope materials with respect to thermal performance, mechanical and hermetic integrity, environmental corrosion resistance and manufacturing risk and cost. Hermetic integrity refers to the ability of a sealed

component to remain leak-tight, preventing any gas or fluid from entering or escaping over time.
Nickel is technically suitable as an envelope material due to its adequate mechanical strength and corrosion resistance. However, its significantly lower thermal conductivity compared to copper and aluminium reduces its effectiveness in heat-transfer-critical applications (The Engineering Toolbox, n.d.). Consequently, it was excluded in order to narrow the selection based on thermal performance criteria.
Titanium was excluded due to its high material cost and challenging fabrication requirements (Protolabs Network, n.d.). Although it offers excellent corrosion resistance and high mechanical strength, these advantages do not justify the increased manufacturing complexity and economic impact within the scope of this study.

Table 8: Elimination matrix for materials.

Material	**Thermal performance**	**Mechanical & Hermetic integrity**	**Environmental corrosion resistance**	**Manufacturing risk & cost**
Al	✓	✓	✓	✓
Cu	✓	✓	✓	✓
SS	✓	✓	✓	✓
Ni	×	✓	✓	✓
Ti	✓	✓	✓	×

Finally, the remaining elements were combined in a morphological matrix, resulting in 28 different concepts, see Table A1. These concepts were then evaluated using a weighted decision matrix, where each concept was assessed based on predefined criteria and their respective importance, see Table A2. All weighting factors together sum to a total of 1. All factors were assigned weights based on Saab's requirements and their assessment of the highest priorities. Thermal performance was assigned the highest weight (0.4), as the primary objective of the system is to achieve efficient heat transfer. Low-temperature performance (0.15) was also considered important to ensure reliable operation under colder conditions, including cold starts. Orientation independence (0.2) reflects the ability of the concept to function effectively regardless of its orientation. High temperature performance (0.15) describes the ability of the system to function effectively at 125°C. Mechanical robustness (0.07) evaluates the structural ability to withstand mechanical stresses during operation. Manufacturability (0.03) considers how easily and feasibly the concept can be produced, it was assigned the lowest weight since it was considered less critical for the objectives of this study. Based on the weighted decision matrix, the ten highest ranked concepts are as follows:

- Concept 22 (4.93)
- Concept 26 (4.87)
- Concept 8 (4.68)
- Concept 12 (4.65)
- Concept 6 (4.53)

- Concept 16 (4.51)
- Concept 2 (4.44)
- Concept 4 (4.44)
- Concept 18 (4.41)
- Concept 20 (4.38)

This will be further discussed and motivated in the next chapter.

5. Concept Results

This chapter presents the results of the concept evaluation process. First, the decision matrix methodology is explained, followed by a comparison of the highest-ranked concepts. Finally, CAD models are introduced to visualize how the selected concepts can be implemented and compared within the same design framework.

5.1 Decision Matrix Methodology

In Table A2, thermal performance was primarily determined by the working fluid, with ammonia providing the best performance across the required temperature range, acetone offering moderate performance, and methanol being less suitable at low temperatures. Further, the wick structure was also considered, where sintered wicks were favored due to their capillary performance, while composite wicks served as the baseline. VC were given slight advantages over CHP due to better heat spreading. Materials played a smaller role, since most of the heat is transferred by the working fluid, where Cu had the highest thermal conductivity, Al had a lower and SS had a much lower thermal performance.

Low temperature performance refers to the ability of the concept to operate reliably at the minimum design temperature at -55°C. It is mainly determined by the thermophysical properties of the working fluid, including freezing point, vapor pressure, and viscosity, together with the wick structure's ability to maintain capillary driven liquid return under increased flow resistance. Other factors include material compatibility and the capacity for the system to withstand freeze cycles without structural degradation. Ammonia was assigned the highest rating due to its excellent low-temperate performance, followed by acetone, which provides moderate suitability, and methanol, with a weaker performance. Sintered wick structures were rated higher than composite wicks. Stainless steel was assigned a lower grade due its reduced thermal conductivity and fabrication challenges under the low-temperature conditions.

Orientation independence was evaluated mainly from the capillary capability of the wick structure. Sintered wicks received the highest rating due to their fine pore structure, which generates high capillary pressure and enables reliable liquid return, independent of orientation. Composite wicks were assigned a lower rating, making them more sensitive to orientation and operating conditions.

The high-temperature performance was evaluated based on the vapor pressure and thermal stability of the working fluid, as well as the structural strength of the material at elevated temperatures. Organic fluids such as acetone and methanol were given higher ratings due to their more moderate pressure characteristics at 125°C, whereas ammonia received a lower rating due to the significantly higher internal pressures it generates. Stainless steel was rated the highest, among the materials, due to its mechanical strength, followed by copper and aluminum.

Mechanical robustness describes the ability of the concept to withstand mechanical and thermal stresses without structural failure. It is influenced by internal pressure, thermal expansion during temperature cycling, geometry, strength of the material and durability of the wick structure. CHP configurations were rated higher due to their stronger geometry and more pressure-resistant properties. Composite wick structures got higher ratings due to their improved tolerance to thermal stresses, especially under thermal cycling. Stainless steel was considered the strongest material under thermal and pressure load, followed by copper and aluminum. Ammonia exhibits significantly higher vapor pressures at elevated temperatures than methanol and acetone, leading to increased internal pressure and greater mechanical loading. Although methanol and acetone do experience rising vapor pressure with temperature, the magnitude is lower, making it less demanding structurally. No concepts were assigned low (1-2) scores in mechanical robustness, as all configurations represent feasible designs.

Manufacturability refers to how easy and realistic a concept is to produce in practice, considering process complexity, material properties, and how well established the manufacturing methods are in industry. The ranking is therefore based on how difficult the different material and wick combinations are to manufacture. Composite wicks can in some cases be considered easier, since the wick structure can be manufactured separately and then integrated into the pipe, which avoids difficult processes such as directly sintering materials like aluminum that have oxide layers. However, for copper, sintering is a well-established and widely used process, making sintered wicks easier to produce than composite ones. This is because they can be manufactured directly inside the pipe with high reliability and fewer additional steps.

The weighted decision matrix involves several inherent trade-offs and therefore does not identify a single concept as universally optimal. The evaluation highlights competing requirements across the considered criteria. Low temperature performance strongly favors ammonia due to its superior vapor pressure characteristics at -55°C, enabling reliable heat transfer. On the other hand, high temperature performance favors acetone and methanol, which exhibit lower vapor pressures at elevated temperatures, resulting in reduced mechanical stress on the structure. Methanol provides significantly lower pressure at high temperatures, although its performance at low temperatures is limited due to insufficient vapor pressure, limiting effective heat transport.

Additionally, structurally strong materials such as stainless steel are advantageous due to their ability to withstand higher internal pressures, at high temperatures. On the contrary, materials with higher thermal conductivity, such as copper and aluminum, improve thermal performance by enhancing heat spreading and reducing thermal resistance. This highlights that improvements in one aspect require trade-offs in another.

5.2 Concept Evaluation

The ten highest ranked concepts from table A2 are presented as following:

1. Concept 22: CHP - Sintered - Acetone - Cu
2. Concept 26: CHP - Sintered - Ammonia - SS
3. Concept 8: VC - Sintered - Acetone - Cu
4. Concept 12: VC - Sintered - Ammonia - SS
5. Concept 6: VC - Sintered - Methanol - Cu
6. Concept 16: CHP - Sintered - Ammonia - Al
7. Concept 2: VC - Sintered - Ammonia - Al
8. Concept 4: VC - Sintered - Acetone - Al
9. Concept 18: CHP - Sintered - Acetone - Al
10. Concept 20: CHP - Sintered - Methanol - Cu

The highest-ranked concepts are all built around sintered wick structures, which consistently deliver strong thermal performance while maintaining good mechanical stability. This makes them particularly effective across a wide operating range, which is reflected in their high weighted scores.

A clear pattern among the top performers is the use of copper and stainless steel in combination with working fluids like acetone and ammonia. Copper-based designs benefit from excellent thermal conductivity, enabling efficient heat transport, while still maintaining robustness through the sintered structure. Stainless steel alternatives have a slightly lower thermal conductivity but compensate with improved structural integrity and compatibility with ammonia, which performs well at higher temperatures.

The difference between CHP and VC configurations is not as important as expected. Both appear in the highest ranks, suggesting that when paired with an effective wick and suitable fluid, either architecture can achieve strong overall performance.

Another clear trend is the strong performance of ammonia-based systems, particularly in stainless steel and aluminum configurations. Ammonia provides reliable high-temperature performance and contributes to good orientation independence, which boosts overall scores despite slightly lower manufacturability in some cases.

Overall, the top concepts stand out because of a balanced combination of thermal efficiency, structural robustness and fluid-material compatibility. It is important to emphasize that the results reflect trade-offs rather than pure feasibility. Concepts that achieve high scores often result from optimizing performance-related criteria, sometimes at the expense of manufacturability and risk. In particular, sintered aluminum concepts, although scoring well, are unlikely to be practical in reality. The sintering process for aluminum is associated with challenges due to oxidation, the need for very precise process control and the difficulties of achieving consistent and reliable structures. These factors make the process both complex and high-risk compared to more established materials like copper or stainless steel. As a result, such concepts should be viewed as theoretically strong but less viable from a manufacturing and implementation perspective. Therefore, only the top five concepts will be taken forward for further evaluation and discussion.

5.3 CAD Model Design

This chapter presents the CAD models developed for the top concepts. The models were designed to be independent of the specific concept combinations meaning that the same geometry could be used for all concepts. This allows a fair comparison between the different configurations within the same design. These concepts were developed to evaluate the heat spreading performance, thermal resistance and overall temperature uniformity.

CAD models of the concepts were developed using Catia V5. The carrier measured 207x140 mm, with a centrally positioned heat source of 60x43 mm. The total assembly thickness for all designs, including all components, remained below 10 mm. Two design ideas were made for the VC concepts, where the size of the VC varied to evaluate the effect of thermal expansion. The CHP concept were designed in a star-shaped configuration to facilitate heat transfer along the carrier, this can be seen in figure 10. The heat pipes had a diameter of 6 mm and were flattened into an elliptical shape, remaining its width of 6 mm but a height of 3 mm. This was done to have a greater surface contact area between the TIM and heat pipes. Both the TIM and the carrier incorporate internal cavities to fit the heat pipes. The grey part represents the solid aluminum carrier, the orange section indicates the VC/heat pipe, the red area marks the heat source, with a green TIM layer located directly beneath it.

Figure 8 illustrates the first VC concept, where the VC covers approximately half of the carrier area (100x140mm). Figure 9 shows the second VC concept, where it covers nearly the entire carrier area (203x136mm).

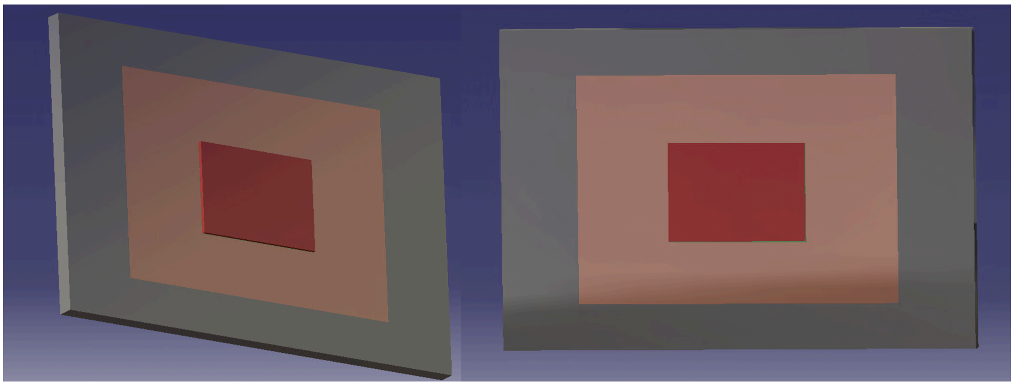

Figure 8: Conceptual design of the 140x100mm VC concept

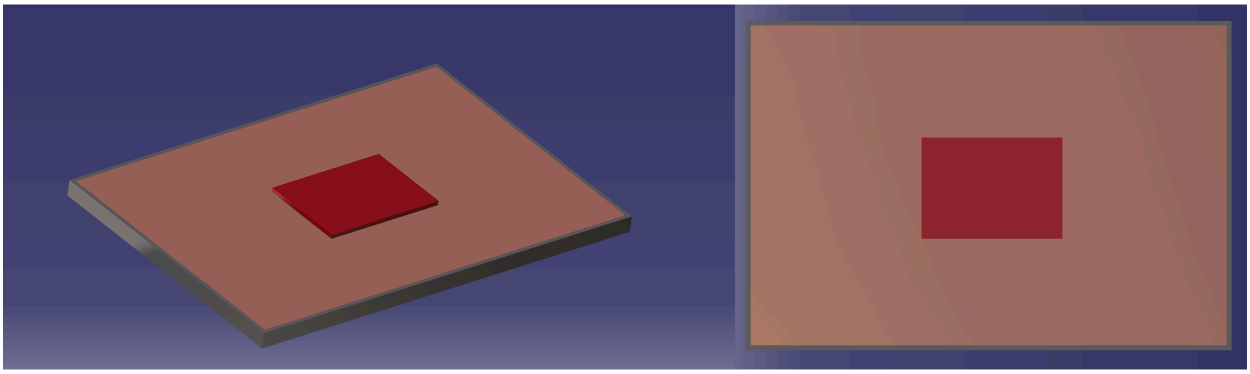

Figure 9: Conceptual design of the 203x136mm VC concept.

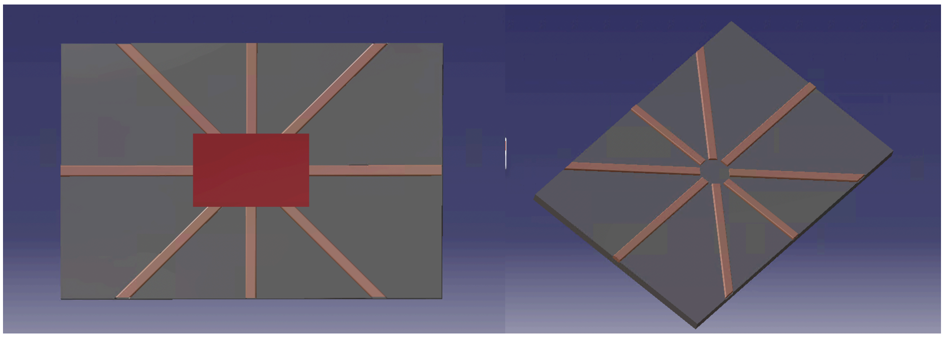

Figure 10: Heat pipe configuration with flattened heat pipes to better fit the TIM and heat source.

6. Simulations

This chapter presents the thermal simulations performed to evaluate the cooling performances of the proposed designs. The objective is to assess how effectively the system dissipates heat from the heat source and to identify any thermal limitations in the design.

6.1 Ansys Icepak

The simulations were performed using Ansys Icepak, a computational fluid dynamics (CFD) tool specialized in cooling electronics. Icepak was used to model the heat source, TIM, heat pipes/vapor chamber, and the surrounding air region. Boundary conditions such as power dissipation, ambient conditions, and gravity were defined to simulate realistic operating scenarios. The heat pipes/VCs were represented using an equivalent anisotropic thermal conductivity to represent their high heat transfer capability.

6.1.1 Boundary Conditions

Boundary conditions were defined to represent realistic operating conditions of the system. The heat source was assigned a constant power dissipation of 200W.

The surrounding domain was modeled as an air region, with openings applied at two opposite sides to allow airflow in and out. One opening was defined as pressure with ambient conditions and the opposite opening was defined as mass flow with a given value of 0.016 kg/s. Natural convection was included in the model by enabling gravity, allowing buoyancy-driven airflow to develop within the air region and transport heat away from the source.

6.1.2 Simulation Result

The models used for the simulations were developed in Catia V5 and shown in the previous chapter. The simulation results are presented in the Figures 11-13.

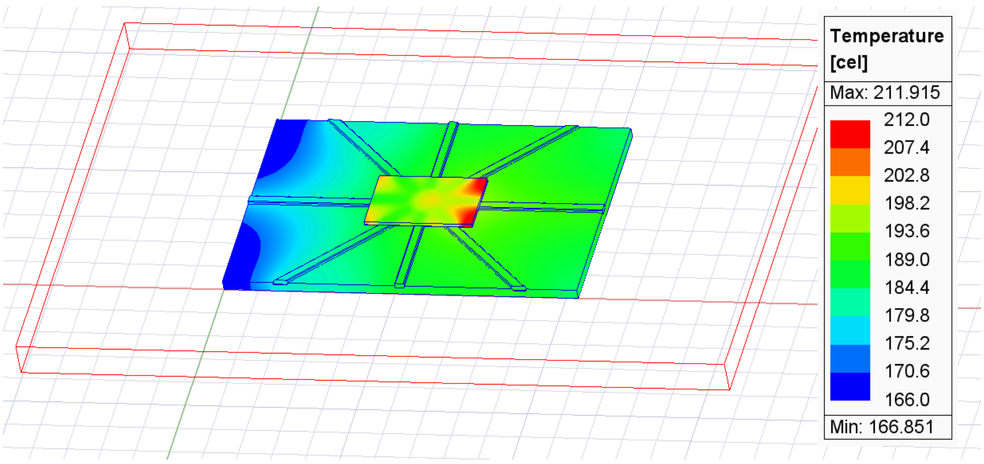

Figure 11: Simulation result of the heat pipe configuration with flattened heat pipes.

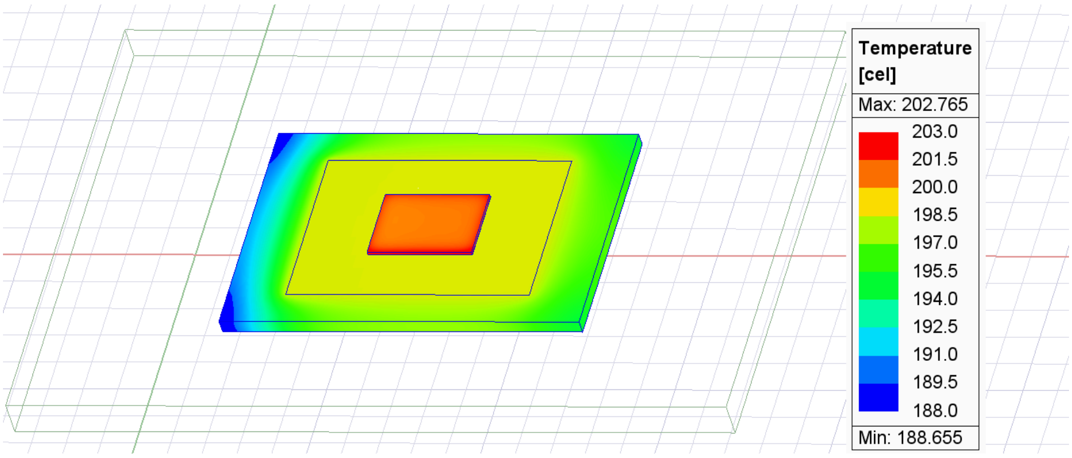

Figure 12: Simulation result of the conceptual design of the 140x100mm vapor chamber concept.

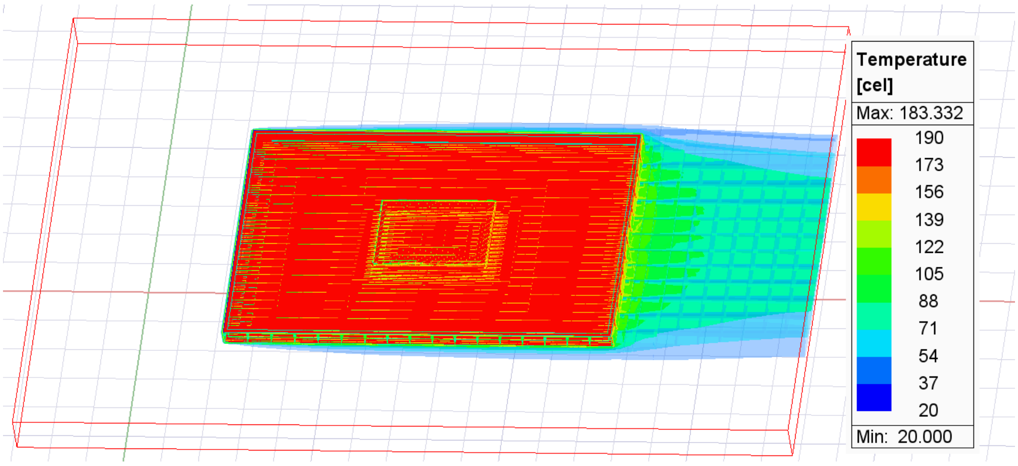

Figure 13: Simulation result of the conceptual design of the 203x136mm vapor chamber concept.

6.1.3 Simulation Analysis

Figure 11 shows that the heat is mainly concentrated around the center heat source, where the highest temperature reaches approximately 212 °C. A clear temperature gradient can be observed from the center toward the outer regions of the model, indicating that the heat pipes transport heat away from the hot spot and distribute it across a larger area. The temperature contours also show that the flattened heat pipes create preferred heat transfer paths, visible as directional cooling patterns extending outward from the center. This suggests that the heat pipes contribute to spreading the thermal load more efficiently compared to pure conduction through the base material alone. However, the result also indicates that the thermal spreading is somewhat non-uniform. Higher temperatures remain concentrated close to the heat source, which implies that the flattened heat pipe configuration still experiences limitations in lateral heat spreading. One possible explanation is that flattening reduces the internal vapor flow area, which increases flow resistance and lowers the overall heat transport capability. This agrees with the theoretical limitations of flattened heat pipes discussed previously in chapter two in the background study.

The simulation result for the 140 × 100 mm VC concept shows a more uniform temperature distribution compared to the flattened heat pipe configuration, see Figure 12. The maximum temperature is approximately 203 °C, which is lower than in Figure 11, indicating improved thermal spreading. The VC distributes the heat laterally across the entire surface, reducing the intensity of the hotspot at the center. This can be observed through the smoother temperature gradients and the larger regions with relatively even temperatures. Compared to the heat pipe configuration, fewer localized hot regions are visible, which suggests that the VC provides a more efficient spreading of heat in two dimensions.

Despite the improved spreading performance, the simulation still shows elevated temperatures near the center heat source. This indicates that although the VC reduces thermal gradients, the total cooling capacity is still limited by the surrounding airflow and boundary conditions.

The result for the larger VC concept should be interpreted with caution, since the simulation setup or result visualization may contain uncertainties, see Figure 13. The figure indicates a lower maximum temperature compared to the previous concepts, but this should not be taken as a fully reliable comparison. Still, the result suggests that increasing the VC area could improve heat spreading and reduce the hotspot temperature. However, further simulations with verified boundary conditions and mesh settings would be needed before drawing a clear conclusion about the performance of this concept.

6.2 Limitations of the Simulation Model

Although Ansys Icepak provided useful insight into the general thermal behavior of the system, several limitations were identified during the simulation work. The software was able to model the heat sink, heat source, airflow and simplified heat pipe. However, the internal two-phase heat transfer mechanisms of the heat pipes and VC could not be modelled accurately within the scope of this study.

In real operating conditions, heat pipes and VCs rely on two-phase heat transfer involving both the working fluid and wick structure. The interaction between the wick structure and the working fluid is essential for the thermal performance of the system. In the simulations, the heat pipes and VC were presented as solid models with anisotropic thermal conductivity. This means that several important factors were not taken into account, including phase change, fluid flow, capillary effects, vapor pressure losses and dry-out conditions. As a result, the simulation was unable to accurately represent the actual thermal performance of the components under realistic operating conditions.

The parameter study showed that the predicted temperatures were more strongly affected by the selected airflow boundary conditions than by the internal transport properties of the heat pipes or vapor chamber. This demonstrated that the simplified model was not sufficient to accurately represent the thermal performance.

Therefore, it was decided not to continue with Ansys simulations and instead, focus more on experimental testing to provide a more realistic presentation with physical measurements. Experimental methods also account for the effects of the wick structure and working fluid, which could not be accurately modeled in the numerical simulations.

7. Experiment

This chapter presents the experimental work that was done. The experiments investigate how copper-water sintered wick heat pipes are affected by different orientations relative to gravity as well as differences in geometry. In addition, two commercially available aluminium-acetone grooved flat heat pipes, called cool pipes, are included in the experiment to broaden the comparison with alternative heat pipe solutions.

Although copper-water heat pipes were not identified as the optimal solution for the specific application, they are widely commercially available and well-documented in literature. This makes them suitable for experimental testing since other heat pipes often need to be custom made, while copper-water heat pipes are readily available and easy to access. The results obtained from these experiments can therefore be used to gain a general understanding of heat pipe behavior which can be applied when evaluating other heat pipe configurations in the project. The cool pipes are also commercially available and represent a more compact flat geometry intended for electronics cooling applications where limited installation space is an important design constraint. Vapor chambers are less standardized and more application-specific, and were therefore not considered in this study since it is more difficult to obtain a general understanding and comparison between different designs.

From the concept selection processes in chapter 5, including elimination matrices and comparison of available heat pipes, it became clear that there is no single heat pipe that fulfills all the project requirements. However, both literature and product analysis show that sintered wick structures are a reliable and well-established solution especially when operation against gravity is required. The cool pipes differ from the copper-water heat pipes by using an aluminium casing, grooved wick structure, and acetone as working fluid, which makes them relevant as an alternative design concept for comparison and confirming the theoretical.

Due to the limited time frame of the thesis, the focus of the experiments is not to find an optimal design but rather to generate comparable and representative data. The goal is to get a general understanding how different heat pipe geometries perform by looking at their thermal resistance. This is relevant as thermal resistance is a simple way to compare different configurations and support design decisions.

The experiment setups have different orientations: gravity-assisted, gravity-opposed and horizontal. This makes it possible to see how gravity affects the liquid return in the wick structure and the overall heat transfer performance. This is of particular interest for the cool pipes since grooved wick structures are generally more sensitive to orientation than sintered wick structures.

All heat pipes, the heat source and the heat sink used in the experiment were commercially purchased components, while the remaining experimental equipment consisted of materials that were available in the laboratory. Both cool pipes were purchased from Farnell (AMEC Thermasol). The round and the flattened heat pipes were purchased from Mouser Electronics. The heat source consisted of a 150W 47Ω power resistor and the heat sink had a thermal resistance of 1 K/W, both obtained from Elfa (Elfa Distrelec). Figure 14 provides an overall illustration of the experimental setup and its main components. Figure 15 shows an illustration of the heat pipe configuration showing the heat sink, TIM, heat pipe, heat source and the two connected thermocouples.

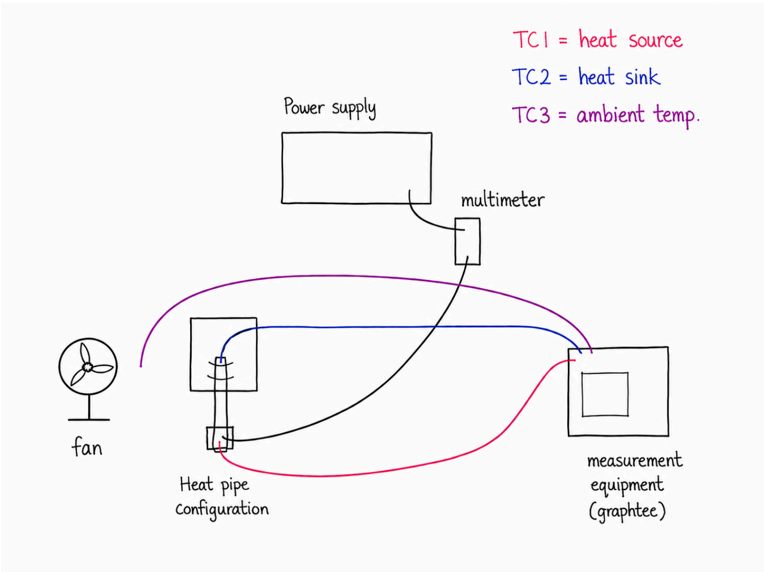

Figure 14: Illustrative figure of the experiment.

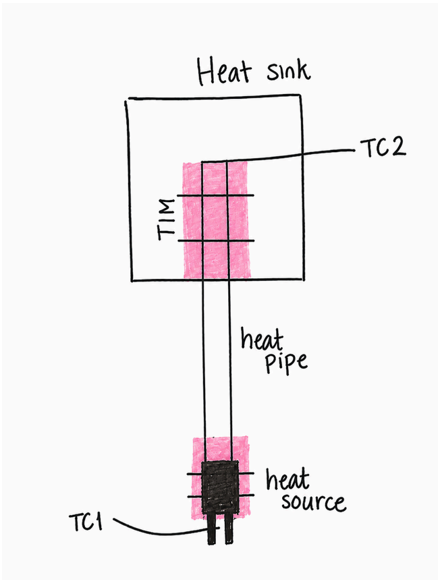

Figure 15: Illustration of the heat pipe configuration.

7.1 Experimental Method

The tested heat pipes are presented in Table 9. For simplicity and to enable comparison in the tables below, the six heat pipes are identified as HP1-6.

Table 9: The different types of heat pipes that were tested.

Heat pipe type	**Wick structure**	**Geometry**	**Dimensions (mm)**
1. Copper-water	Sintered	Cylindrical	Ø6 × 250
2. Copper-water	Sintered	Cylindrical	Ø8 × 250
3. Copper-water	Sintered	Flattened	8.2 × 2.5 × 250
4. Copper-water	Sintered	Flattened	10.5 × 4.5 × 250
5. Cool pipe (aluminum-acetone)	Grooved	Flat	200 × 40 × 2
6. Cool pipe (aluminum-acetone)	Grooved	Flat	200 × 50 × 2.5

The following equipment and materials were used to assemble the experimental setup.

Materials:

- Heat sink
- Heat source
- Thermocouples
- Cooling fan
- Data acquisition system (GraphTec)
- Power supply
- Cable ties
- Thermal interface material (TIM) -two types
- Heat pipe - six types
- Electrical cables

Figure 16 shows the complete experimental setup on a laboratory bench. The setup consists of the heat sink and heat pipe assembly, a power supply used to provide controlled heating and measurement equipment (GraphTec) connected to several sensors for monitoring the thermal behaviour of the system during testing. Three K-type thermocouples were used to record temperatures at different locations, one measured the ambient air temperature, one was attached to the evaporator end at the heat source and the third was attached between the condenser end and the heat sink to monitor the temperature distribution along the heat pipe. A fan with 3W was placed approximately 15cm from the heat sink to provide assisted cooling.

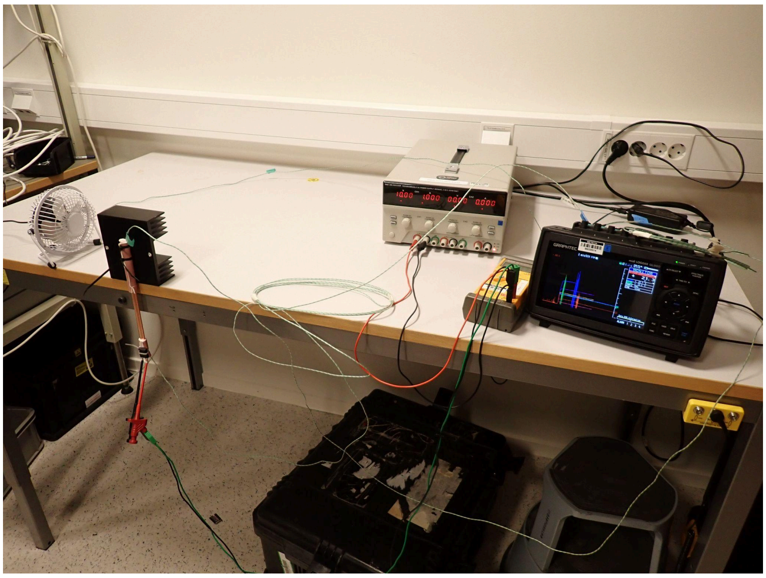

Figure 16: Experimental setup

The heat sink was fitted with pre-drilled holes that allowed cable ties to securely fasten the heat pipe in place. A TIM with a thermal conductivity of 1 W/mK was applied around the heat pipe to improve thermal contact with the heat sink before fastening. At the opposite end of the heat pipe, the heat source with a resistance of 47Ω was mounted with an additional TIM layer between the surfaces to ensure efficient heat transfer. For the flat heat pipes, the TIM with 1 W/mK was used at both ends and for the cylindrical heat pipes a different TIM with the thermal conductivity of 10 W/mK was used. The cylindrical heat pipes had a more moldable TIM to ensure maximum contact with the heat sink and heat source, this can be seen in Figure 17 below. In all cases except the cool pipes, the TIM was surrounding the heat pipe to ensure isolation. For the cool pipes, the TIM between the heat pipe and heat source was only applied over an area approximately equal to the size of the heat source itself. It was unnecessary to surround the pipe with the TIM, since the heat source was smaller than the pipe, in contrast to the heat pipes, this can be seen in Figure 22. The heat source was attached to the heat pipe with electrical tape that withstands temperatures up to 180°C.

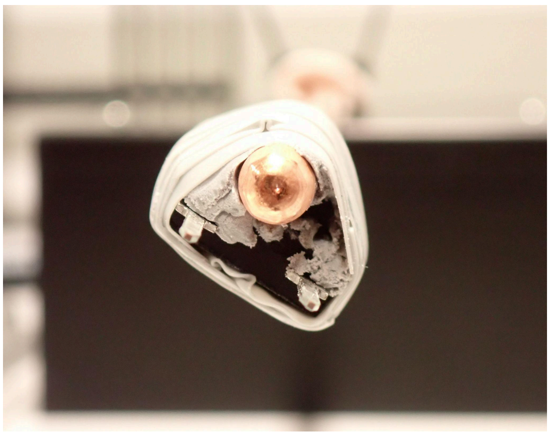

Figure 17: Moldable TIM applied to cylindrical heat pipe.

Each heat pipe was tested in three different orientations relative to gravity: gravity assisted, gravity opposed and horizontal, as shown in the following figures, Figure 18-21. In the sgravity assisted orientation, the condenser was positioned above the evaporator to support the liquid return. In the gravity opposed orientation, the evaporator was positioned above the condenser, forcing the wick structure to transport the liquid against gravity. In the horizontal orientation, gravitational effects on the liquid return were minimized.

The electrical power supplied to the heater was controlled by adjusting the output voltage of the DC power supply, while the current adjusted according to the electrical resistance of the heater. During the initial tests, an applied voltage of 5V resulted in only a minor temperature increase and was therefore considered negligible. Consequently, 10V was selected as the starting point for the remaining experiments. The experiments were then carried out at 10V, 20V and 30V, corresponding to heat inputs of roughly 2W, 8W and 19W, respectively. Before increasing the voltage level, the system was allowed to reach steady-state conditions to ensure stable temperature measurements. Steady state was typically reached after 10-20 minutes, after which the temperatures were recorded using the GraphTec logger throughout the experiments.

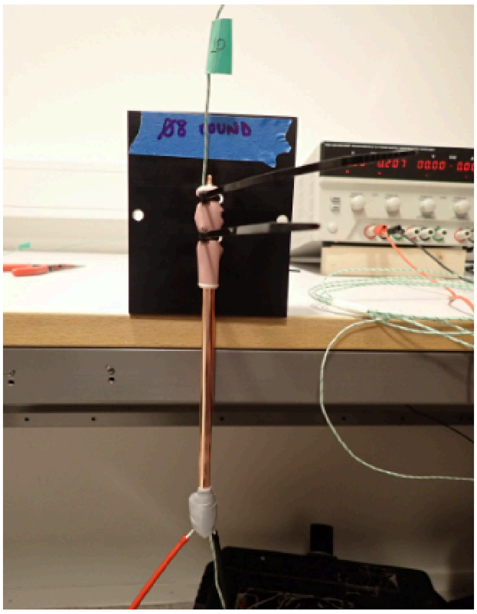

Figure 18: Gravity assisted setup.

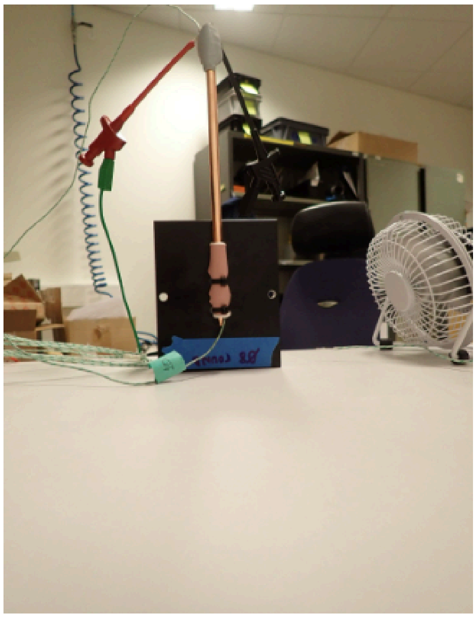

Figure 19: Gravity opposed setup.

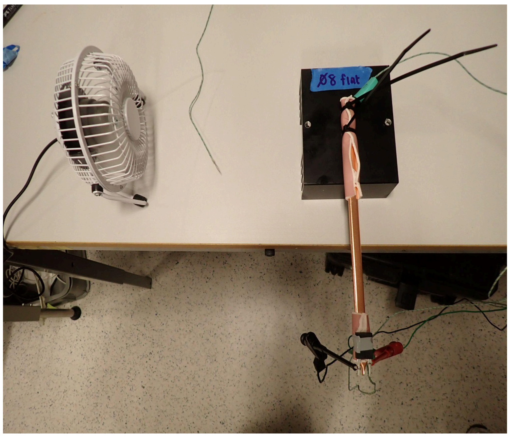

Figure 20: Horizontal setup.

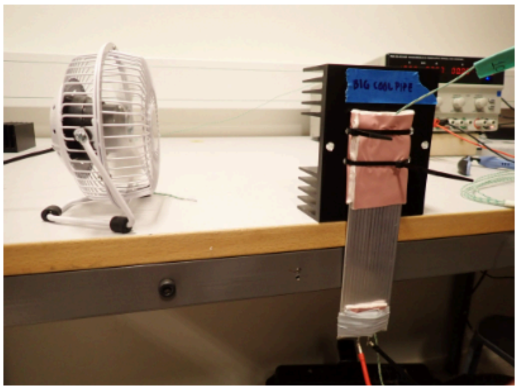

Figure 21: Gravity assisted cool pipe setup.

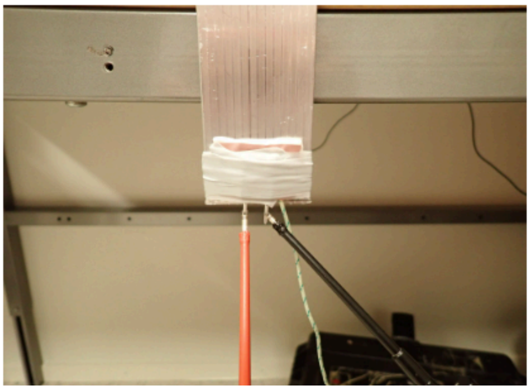
Figure 22: Close-up on the heater fastening.

After the experiments, the temperatures at the evaporator and condenser were compared to evaluate the thermal performance of the different heat pipe setups. The thermal resistance was calculated using Equation 1.

$$R_{th} = \frac{T_1 - T_2}{Q} \tag{1}$$

where T_1 was the temperature at the heat source, T_2 was the temperature at the heat sink and Q was the total power. A higher thermal resistance is undesirable since it indicates poorer heat transfer within the system. In heat pipes, a high thermal resistance means that a larger temperature difference is required between the heat source and the heat sink to transfer the same amount of heat. As a result, the temperature at the evaporator becomes higher, which decreases the efficiency of the cooling process and increases the risk of overheating or dry-out conditions. Therefore, a lower thermal resistance is preferred, as it indicates more effective heat transfer and better thermal performance.

7.2 Experimental Results

The experimental results were obtained at three different power levels: 2W, 8W and 19W. For each voltage level, temperatures were recorded at three measurement points using thermocouples (TC). Since the ambient temperature remained relatively constant between 22.0-22.5°C throughout the entire experiment, the TC3 values are not included in Tables 10-15 and A3-A5. The tables include the thermal resistance, denoted by R_{th}. All thermal resistance for the tables 13-15 was calculated with Q = 19W, and Q = 8W for Table 10-12.

Tables 10-12, present the recorded temperatures for each heat pipe at 8W and 19W in the gravity assisted, gravity opposed and horizontal setup. To enable comparison, each table corresponds to one specific orientation of the heat pipes. The recorded temperatures at 2W with corresponding orientations can be seen in Tables A3-A5 in the appendix. The entries marked with "-" indicate the runs that were terminated before reaching steady-state conditions. In these cases, the temperature profile increased rapidly, leading to potentially unsafe operating conditions, and the runs were therefore cancelled to avoid damaging the system or compromising safety. This behaviour is illustrated in figures 25-26 further down in this chapter.

Table 10: Temperature measurements at 8W in the gravity assisted setup.

Heat Pipe	TC1 – Heat Source (°C)	TC2 – Heat Sink (°C)	ΔT (TC1–TC2)	R_{th} (°C/W)
HP1	57.5	45.2	12.3	1.54
HP2	35.8	28.3	7.5	0.94
HP3	46.0	41.8	4.2	0.53
HP4	48.7	34.0	14.7	1.84
HP5	69.0	31.3	37.7	4.71
HP6	48.5	29.5	19.0	2.38

Table 11: Temperature measurements at 8W in the horizontal setup.

Heat Pipe	TC1 – Heat Source (°C)	TC2 – Heat Sink (°C)	ΔT (TC1–TC2)	R_{th} (°C/W)
HP1	46.7	34.2	12.5	1.56
HP2	33.0	26.5	6.5	0.81
HP3	36.8	35.0	1.8	0.23
HP4	37.3	28.7	8.6	1.08
HP5	62.1	28.0	34.1	4.26
HP6	36.0	28.5	7.5	0.94

Table 12: Temperature measurements at 8W in the gravity opposed setup.

Heat Pipe	TC1 – Heat Source (°C)	TC2 – Heat Sink (°C)	ΔT (TC1–TC2)	R_{th} (°C/W)
HP1	50.5	40.0	10.5	1.31
HP2	36.6	30.0	6.6	0.83
HP3	47.1	37.3	13.4	1.68
HP4	40.6	32.1	8.5	1.06
HP5	-	-	-	-
HP6	80.0	26.2	53.8	6.73

The following tables, Tables 13-15, present the recorded temperatures for each heat pipe at 19W in the gravity assisted, gravity opposed and horizontal setup.

Table 13: Temperature measurements at 19W in the gravity assisted setup.

Heat Pipe	TC1 – Heat Source (°C)	TC2 – Heat Sink (°C)	ΔT (TC1–TC2)	R_{th} (°C/W)
HP1	-	-	-	-
HP2	54	35	19	1.00
HP3	65.8	58.9	6.9	0.36
HP4	71.0	44.0	27	1.42
HP5	-	-	-	-
HP6	73.8	35.5	38.3	2.02

Table 14: Temperature measurements at 19W in the horizontal setup.

Heat Pipe	TC1 – Heat Source (°C)	TC2 – Heat Sink (°C)	ΔT (TC1–TC2)	R_{th} (°C/W)
HP1	74.3	48.9	25.4	1.34
HP2	46.5	30.3	16.2	0.85
HP3	51.5	50.5	1.0	0.05
HP4	55.5	37.2	18.3	0.96
HP5	-	-	-	-
HP6	53.0	35.1	17.9	0.94

Table 15: Temperature measurements at 19W in the gravity opposed setup.

Heat Pipe	TC1 – Heat Source (°C)	TC2 – Heat Sink (°C)	ΔT (TC1–TC2)	R_{th} (°C/W)
HP1	-	-	-	-
HP2	57.7	38.0	19.7	1.04
HP3	-	-	-	-
HP4	62.1	45	17.1	0.90
HP5	-	-	-	-
HP6	-	-	-	-

The plots shown in Figures 23-25 illustrate the performance of HP3 in all orientations at each voltage level. The red curve represents the temperature at the heat source, the blue curve represents the heat sink and the green curve represents the ambient temperature. Figure 27 shows the heat source after it melted during the experiment. A possible explanation is that there was inefficient thermal contact between the heat source and heat pipe, which may have been caused by misalignment. Figures 23-26 and Figure 28 display time on the x-axis and temperature on the y-axis.

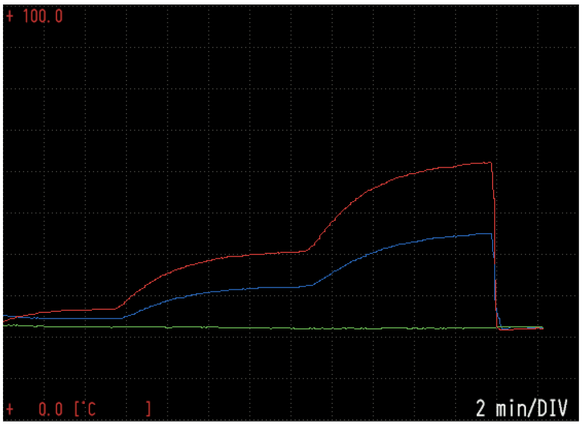

Figure 23: HP3 at gravity assisted position.

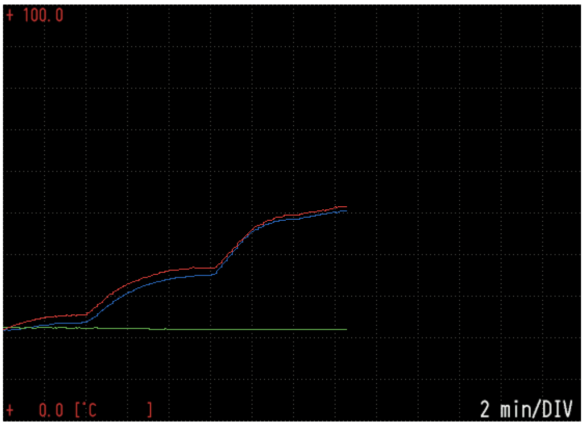

Figure 24: HP3 at horizontal condition.

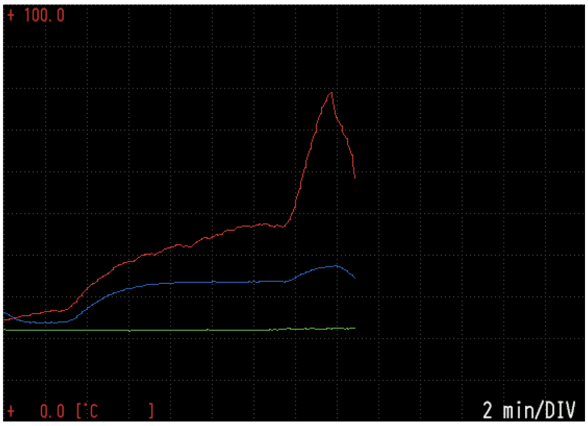

Figure 25: HP3 at gravity opposed position.

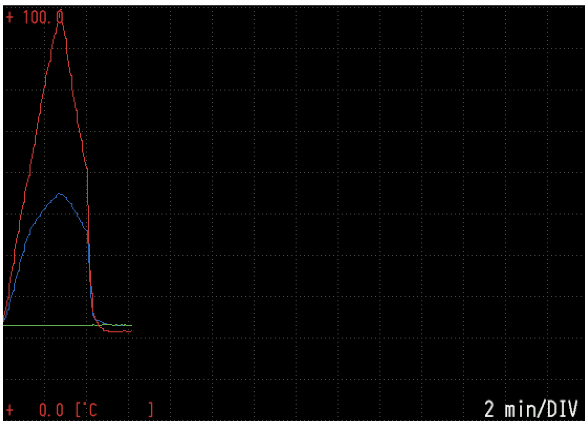

Figure 26: Second trial of HP3.

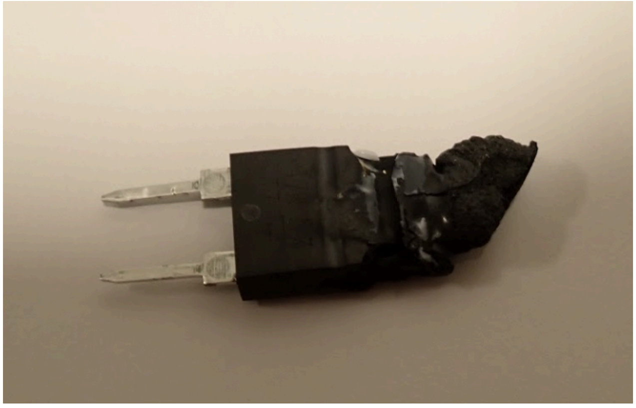

Figure 27: Melted heat source

Figure 28, illustrates HP6 (aluminum, acetone cool pipe) and its sudden temperature dip at approximately 73°C.

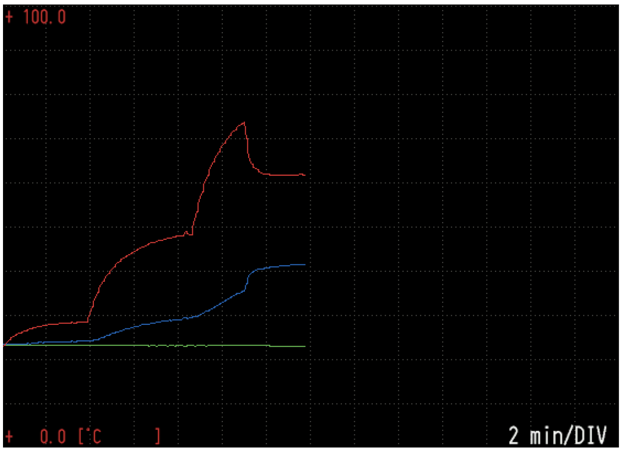

Figure 28: Deviating plot for HP6 at gravity assisted.

7.3 Experimental Analysis

This chapter further discusses and analyses the results obtained from the experiments.

7.3.1 Gravity-assisted Setup

At 8 W in the gravity assistance, as seen in Table 10, HP1 and HP2 showed thermal resistance values of 1.54 °C/W and 0.94 °C/W, respectively. These values are considered reasonable for a simple experimental setup operating under ambient conditions and without thermal insulation. Since HP1 and HP2 were cylindrical copper-water heat pipes with sintered wick structures, they were theoretically expected to provide good thermal performance. However, the cylindrical geometry also resulted in a limited contact area between the heat pipe surface and the flat heater resistor. The heat source was mounted externally using TIM and fastened with electrical tape, the thermal contact was not completely flush which likely increased the contact resistance and therefore the measured thermal resistance values.

The flattened copper-water heat pipes, HP3 and HP4, achieved thermal resistance values of 0.53 °C/W and 1.84 °C/W, respectively. The lower value measured for HP3 indicates more effective heat transfer compared to the cylindrical heat pipes. A likely explanation is that the flattened geometry provided a larger and more uniform contact surface against both the heater and the heat sink, resulting in improved thermal contact and lower contact resistance. HP4, despite also being flattened, showed a higher thermal resistance value. This may be related to differences in geometry, flattening dimensions, mounting pressure or TIM distribution during assembly, which could have affected the thermal contact conditions.

HP5 and HP6, which were the aluminium-acetone cool pipes with grooved wick structures, showed thermal resistance values of 4.71 °C/W and 2.38 °C/W. Compared to the copper-water heat pipes, these values indicate less effective heat transfer performance. HP6 still showed stable operation, although with a noticeably higher thermal resistance, while HP5 performed significantly worse than all other tested configurations. One possible explanation is that the thin flat geometry of the cool pipes made the thermal contact conditions more sensitive to mounting pressure and TIM distribution. In addition, the grooved wick structure may not have distributed the working fluid as effectively as the sintered wick structures used in the copper-water heat pipes, even in the gravity assisted orientation.

At 19 W in the gravity assisted setup, also seen in Table 13, only HP2, HP3, HP4 and HP6 maintained stable operation throughout the experiments. Compared to the results at 8 W, several heat pipes showed improved thermal resistance values, indicating that the heat transfer performance became more effective at the higher heat load. This behavior is reasonable since heat pipes generally operate more efficiently enoguh evaporation and vapor flow have been established inside the structure.

HP1 did not provide stable measurements at 19 W. Since HP1 was theoretically expected to perform better than the measured results at 8 W, and considering the relatively large temperature difference already observed at the lower heat load, it is likely that the failed 19 W test was caused by variations in mounting conditions or human error during assembly rather than limitations of the heat pipe itself. A potential source of human error could be inconsistencies in the placement and applied pressure of the TCs on the heat pipes.

The thermal resistance value for HP2 was 1.00 °C/W, which is similar to the value measured at 8 W. The cylindrical geometry still likely limited the thermal contact area against the flat heater surface, resulting in additional contact resistance within the setup. Nevertheless, the heat pipe maintained stable operation and showed reasonable thermal performance under the increased heat load.

HP3 achieved the lowest thermal resistance value of all tested configurations at 0.36 °C/W. This indicates highly effective heat transfer in the gravity-assisted setup. Similar to the 8 W case, the flattened geometry likely improved the contact conditions against both the heater and the heat sink, reducing thermal contact resistance and improving the overall heat transfer performance.

The R_{th} value for HP4 was lower than the value measured at 8 W but still significantly higher than HP3. Since both HP3 and HP4 were flattened copper-water heat pipes with sintered wick structures, the difference in performance may again be related to geometry, mounting conditions or variations in thermal contact during assembly.

HP6 showed a thermal resistance value of 2.02 °C/W, which was still higher than the copper-water heat pipes. Although stable operation was maintained, the results indicate less effective heat transfer performance under the tested conditions, likely due to the grooved wick structure and thin flat geometry.

7.3.2 Horizontal Setup

The lower thermal resistance values observed in the horizontal orientation were somewhat unexpected, since gravity-assisted operation is generally considered beneficial for heat pipe performance. This can be seen in Table 11. However, at the relatively low heat load of 8 W, the wick structures were likely capable of maintaining sufficient liquid return even without the help of gravity. Since the tested heat pipes were also relatively short, the internal capillary forces were likely sufficient to sustain stable operation in the horizontal orientation. Under these conditions, external factors such as thermal contact resistance, TIM distribution and mounting conditions may therefore have had a larger influence on the measured thermal resistance than gravity itself.

This behavior can be seen for several of the tested heat pipes. HP2 showed a slightly lower thermal resistance in the horizontal setup compared to the gravity assisted setup, while HP3 achieved the overall lowest thermal resistance value. HP4 also improved noticeably in the horizontal orientation. Since HP3 and HP4 were flattened heat pipes, the larger contact area against both the heater and heat sink likely contributed to the improved performance. HP6 also showed a significant decrease in thermal resistance in the horizontal setup, suggesting that the grooved wick structure worked more effectively when the liquid return distance remained small. HP5, however, continued to show poor thermal performance in all tested orientations, indicating that the limitations were likely related to the geometry or internal structure rather than the gravitational orientation itself.

At 19 W in the horizontal setup, HP3 showed the best overall performance with a thermal resistance of only 0.05 °C/W, this is observed in Table 14. The very small temperature difference between the heat source and heat sink indicates highly effective heat transfer. Similar to the 8 W results, the flattened geometry likely improved the contact against both the heater and the heat sink, reducing contact resistance within the setup.

HP2 and HP4 also showed relatively low thermal resistance values of 0.85 °C/W and 0.96 °C/W, respectively, indicating stable operation at the higher heat load. Compared to HP1, these heat pipes appeared less affected by contact limitations within the setup. HP1 showed a higher thermal resistance of 1.34 °C/W, which was likely influenced by the cylindrical geometry and the limited contact area against the flat heater surface.

HP6 showed a clear improvement compared to the gravity-assisted setup, where the thermal resistance decreased from 2.02 °C/W to 0.94 °C/W. This suggests that the cool pipe operated more effectively in the horizontal orientation at 19 W. HP5 did not provide stable measurements and the test was therefore not included in the comparison.

7.3.3 Gravity-opposed Setup

In Table 12, it is observed that the gravity-opposed R_{th} values generally increased compared to the other orientations meaning reduced heat transfer performance. This behavior was expected since the wick structures must generate enough capillary pressure to transport the liquid back to the evaporator while working against gravity. Despite this, HP1 and HP2 still maintained relatively low in their values. This suggests that the cylindrical sintered heat pipes were capable of stable operation. HP2 again showed better performance than HP1, likely due to the same reason as for the other orientations.

For HP3 and HP4, the R_{th} values increased meaning that the flattened geometry may have become more sensitive to liquid return limitations. However, HP4 remained relatively stable and had a smaller decrease in performance.

HP6 showed the largest increase in thermal resistance, reaching 6.73 °C/W, which was by far the highest measured value among the heat pipes. The grooved wick struggled to return enough working fluid against gravity, resulting in the large temperature difference between the evaporator and condenser. This behavior is consistent with the expected orientation sensitivity of grooved wick. HP5 did not produce stable measurements in the gravity-opposed setup and the test was therefore aborted. During the experiment, the evaporator temperature increased rapidly while the condenser temperature showed little response, indicating that the heat pipe likely stopped transferring heat effectively. This behaviour may suggest partial dry-out or insufficient liquid return within the grooved wick structure. A possible reason is the smaller dimensions of HP5 compared to HP6.

Table 15 illustrates 19 W in the gravity opposed setup, only HP2 and HP4 completed the experiments with stable measurements. The measured thermal resistance values of 1.04 °C/W and 0.90 °C/W indicate that both heat pipes were still capable of transporting heat effectively despite operating against gravity. HP4 showed the lowest thermal resistance, which may be related to the improved surface contact provided by the flattened geometry.
The remaining heat pipes did not maintain stable operation at this heat load. For HP5 and HP6, this was expected due to the grooved wick structures, which are generally less effective when the working fluid must return against gravity. The failed tests for HP1 and HP3 were more unexpected and were likely influenced by experimental uncertainties such as mounting conditions or thermal contact variations during assembly.

In conclusion, although HP3 achieved lower thermal resistance values in some cases, HP4 demonstrated more stable and predictable behaviour throughout the experiments. Since no major deviations or sudden performance changes were observed, the HP4 results are considered among the most reliable measurements obtained in this study.

7.3.4 Plot Analysis

As observed in Figures 23-24, it is clear that the system reached steady-state conditions in a stable and controlled way. Although the results obtained in Figure 23 were promising, the shell surrounding the heat source melted during the experiment while it was at 30V. Although this behaviour seemed unusual and was not repeated at higher temperatures, it did not appear to significantly influence the measured results. The damaged heat source can be seen in Figure 27. However, Figures 25-26 shows that the temperature measured at the heat source increased sharply, without a similar response from the TC at the heat sink. The sharp decrease in Figures 25-26 does not represent normal behavior, the experiments were stopped to avoid damaging the system, and the drop corresponds to the cooling phase after shutdown. The temperature spikes because the heat pipe reaches a dry-out condition. When placed against gravity, the wick cannot return enough liquid back to the evaporator, leading to rapid overheating at the evaporator while the heat sink temperature changes only slightly. The experiment for HP3 at gravity opposed position was repeated twice to verify the results, as illustrated in Figure 26.

Figure 28 shows HP6 and the sudden temperature dip observed at approximately 73 °C. This was likely caused by the heat pipe entering a more effective two-phase operating state. At this point, enough acetone had vaporized to enhance the internal circulation of the working fluid. Since the heat pipe was operating in the gravity-assised orientation, the condensate could return more effectively to the evaporator through the grooved wick. As a result, the heat source temperature decreased and the heat sink temperature increased correspondingly.

8. Results and Discussion

The theoretical results showed that sintered wick structures dominated the highest-ranked concepts, indicating that wick structures are one of the most important parameters for achieving strong overall thermal performance. Since sintered wicks provide a balance between capillary performance, heat transfer capability and mechanical stability, they scored highly across both VC and CHP configurations.

The material and working fluid combinations play a major role as well. Copper-based concepts perform strongly due to copper's high thermal conductivity, which improves heat transport efficiency. Stainless steel concepts rank highly, especially when paired with ammonia, since they offer better structural robustness and compatibility with higher operating temperatures. The key takeaway from the theoretical analysis highlights the importance of trade-offs during concept selection. The highest ranked concepts are not necessarily the most practical or manufacturable solutions. Several aluminum-based sintered concepts achieved strong scores, but real world feasibility is limited due to the challenges associated with sintering aluminum. Overall, the results suggest that the strongest concepts are not those that maximize a single parameter, but those who achieve a balanced combination of all desired parameters.

The experimental results showed that sintered wick heat pipes perform better than grooved wick heat pipes, particularly in non-gravity assisted orientations. In addition, larger heat pipes demonstrated better thermal performance compared to smaller heat pipes of the same type. This improvement is due to the larger contact area, which also confirms the theoretical expectations presented in the background study. As stated in the theoretical study, acetone performs better at higher temperatures, which was also confirmed by the experimental results.

As shown in Figure 28, the acetone-based heat pipe activates at a certain temperature, after which its thermal performance becomes significantly more effective.

The flattened heat pipes generally achieved lower thermal resistance values than the cylindrical heat pipes, likely due to the larger contact area against the heat source and heat sink. HP3 demonstrated the best overall thermal performance at both 8W and 19W. However HP4 was considered to be the most reliable due to minimal deviations in performance throughout the test. The results also showed that thermal resistance generally increased in the gravity-opposed orientation, indicating reduced heat transfer performance when the working fluid had to return against gravity. At the higher heat load of 19W, the majority of the heat pipes were unable to maintain stability in this orientation. Although some experimental uncertainties were present, the results generally agreed with the theoretical expectations.

It should also be noted that the evaluation and testing were performed under simplified conditions, where the concepts were analyzed as single components, rather than integrated into a complete system. In a real application, the assembly would be fully integrated in a system, together with surrounding components, interfaces and packaging limitations, which could significantly affect its thermal behavior and overall performance. Parameters such as contact resistance, airflow conditions, mechanical constraints and interactions with neighboring components may alter the behavior of the concepts compared to the results obtained in the current study.

8.1 Limitations and Sources of Errors

A potential source of error in the experimental setup was the mounting consistency of the heat pipes on the heat sink. The heat pipes may have not been positioned identically during each test and the fastening pressure likely varied between testes due to differences in TIM thickness and geometry.

Another source of error was the application of the TIM itself. The TIM was not applied with identical size and distribution for every heat pipe, which may have affected the thermal contact resistance. In some cases, gaps were present between the contact surfaces, while in others, the TIM overlapped itself. Additionally, two different types of TIMs were used for the round and flat heat pipes. Since these TIMs had different thermal conductivities, they may have also contributed to variations in the measured thermal performance.

Another source of uncertainty in the experiments was the thermocouple positioning. The thermocouples attached at the heat source and heat sink were sensitive to small positional changes, and even minor movement during the experiments could affect the measured temperatures. Since the sensors were mounted externally on the surface of the heat pipes and heat sink, slight variations in contact position or pressure may have introduced measurement deviations and influenced the calculated thermal resistance values. In addition, the orientation of the heat pipe may not have been perfectly identical between tests. Minor deviations in angles could influence the fluid return mechanism, in all orientations due to the fact that orientation has a significant effect on overall performance.

Further sources of errors were related to the experimental environment and setup conditions. Since the setup was exposed to the surrounding environment, some heat losses to the ambient air were unavoidable, meaning that not all supplied heat was transferred through the heat pipe. Since none of the components were mounted in the setup, variations in airflow conditions were unavoidable. Small differences in fan position, airflow direction or local air circulation around the setup may have influenced the cooling conditions and therefore the temperature measurements. Another variable that may have affected the results could be the variations in room temperature. However, since the room temperature remained relatively stable throughout the experiments, with a maximum variation of approximately 1°C, the impact of this factor remains limited.

9. Conclusions

The aim of this thesis was to investigate whether passive two-phase heat transfer devices could be used in airborne applications. Based on the theoretical evaluation, concept comparison and experimental work performed in this study, the results indicated that passive heat pipe solutions were technically feasible for this type of application. However, the work also showed that there was no single heat pipe configuration that optimized all desired properties at the same time. Instead, the suitability of a concept depended on achieving a balance between thermal performance, manufacturability, orientation independence and structural robustness.

The theoretical concept evaluation showed that wick structure was one of the most important design parameters for airborne heat pipes. Sintered wick structures were considered the strongest among the concepts due to their high capillary pressure even under varying orientations. This became especially important since the intended application involved operation in both gravity-assisted and gravity-opposed conditions. The evaluation of the concepts also showed the importance of choosing the best combination of working fluid and envelope material. Copper-based concepts showed strong thermal performance due to copper's high thermal conductivity, while stainless steel concepts provided improved structural robustness, especially in combination with ammonia at higher temperatures.

The experimental work generally confirmed the theoretical expectations from the background study and concept evaluation. Sintered wick heat pipes demonstrated better thermal performance than grooved wick heat pipes, especially in non-gravity-assisted orientations. The experiments also showed that flattened heat pipes generally achieved lower thermal resistance values compared to cylindrical heat pipes due to improved contact area against the heat source and heat sink. In addition, larger heat pipes demonstrated improved thermal performance compared to smaller heat pipes of similar design. The results also showed that orientation has a big influence on heat pipe performance. Most heat pipes experienced increased thermal resistance during gravity-opposed operation, particularly at higher heat loads where several setups became unstable.

The study also showed the importance of considering manufacturability and integration during the concept selection process. Some concepts had good theoretical performance but were not considered realistic to manufacture. The work also showed that surrounding integration conditions, such as thermal interfaces and mounting conditions can have a large impact on the final system performance.

In conclusion, the results of this thesis showed that passive two-phase cooling systems were promising alternatives for future airborne applications. Among the investigated concepts, sintered wick heat pipes and vapor chamber concepts appeared to be the most suitable options. However, future work is needed to study the performance under realistic airborne conditions such as vibration, acceleration loads and long-term operational reliability.

10. Recommendations and Future Work

Although the thesis shows that passive two-phase heat transfer devices are promising for airborne applications, there are still areas that require further investigation before they can be used in real systems. Future work should include experimental investigations of VC concepts, as the theoretical analysis identified them with strong potential. Further studies should also focus on more integrated cooling designs, where the heat spreader is evaluated within a complete system instead of as a standalone component. Overall, there should be more testing of realistic conditions, such as including vibration, acceleration loads and long-term reliability testing. Investigations like these are important for evaluating the system in real applications and not only theoretical.

Future experiments should also include testing the heat pipe concept that was identified as the highest performing in the theoretical evaluation, rather than limiting the study to commercially available heat pipes. This would allow a more representative validation of the highest ranked concepts and enable optimization of all parts within the heat pipe specifically for airborne conditions.

Another possible direction is to further investigate copper-water heat pipes, since they are already well established and commonly used in electronics cooling. Even though water was eliminated in the theoretical concept selection due to its freezing point, the experimental results showed that copper-water heat pipes can still provide strong thermal performance once the working fluid is in the operating range. Future work could therefore study how freeze-thaw limitations could be managed in airborne applications. One possible solution would be to integrate a small heater or pre-heating strategy to ensure that the working fluid is thawed before full heat pipe operation is required. Another alternative would be to investigate a hybrid thermal management concept. In such a system, a secondary heat transfer path or an additional heat pipe using a low-temperature working fluid could support cooling during cold start conditions. Once the copper-water heat pipe reaches its operating temperature, it could then take over as the main heat transfer device. This type of combined solution could make it possible to benefit from the high thermal performance and availability of copper-water heat pipes while reducing the limitations caused by freezing at low temperatures.

11. References

Advanced Cooling Technologies (ACT). (n.d.). Heat Pipes 101. https://www.1-act.com/thermal-solutions/passive/heat-pipes/heat-pipes-101/?srsltid=AfmBOorhBlMk4G5qOP_mYH44dNskqtI-rEtwIQIrA1ah9YEPnDwE39hl
Advanced Thermal Solutions, Inc (ATS). 2013. The Impact of Orientation on a Heat Pipe's. https://www.qats.com/?utm_source=Qpedia&utm_medium=Download&utm_campaign=Qpedia_ad_hatching

AMEC Thermasol. (n.d.). MHP-2550A200A heat pipe, flat, 200 mm × 50 mm × 2.5 mm. Farnell. Retrieved May 10, 2026, from Farnell. https://se.farnell.com/amec-thermasol/mhp-2550a200a/heat-pipe-flat-200mmx50mmx2-5mm/dp/3972216

AMEC Thermasol. (n.d.). MHP-2040A200A heat pipe, flat, 200 mm × 40 mm × 2 mm. Farnell. Retrieved May 10, 2026, from Farnell. https://se.farnell.com/amec-thermasol/mhp-2040a200a/heat-pipe-flat-200mmx40mmx2mm/dp/3972210

Arab, M., & Abbas, A. (2014). A model-based approach for analysis of working fluids in heat pipes. Applied Thermal Engineering, 73(1), 751–763. https://doi.org/10.1016/j.applthermaleng.2014.08.001

Atay, A., Sariarslan, B., F. Kuscu, Y., Saygan, S., Akkus, Y., Gurer, T., Cetin, B., & Dursunkaya, Z. (2019). PERFORMANCE ASSESSMENT OF COMMERCIAL HEAT PIPES WITH SINTERED AND GROOVED WICKS UNDER NATURAL CONVECTION. Orta Doğu Teknik Üniversitesi. https://www.researchgate.net/publication/336680193_Performance_Assessment_of_Commercial_Heat_Pipes_with_Sintered_and_Grooved_Wicks_Under_Natural_Convection

Boyd Corporation. (2022). Two-phase thermal solution guide: A quick & easy reference to two-phase cooling technologies. https://info.boydcorp.com/hubfs/Thermal/Two-Phase-Cooling/Boyd-Two-Phase-Cooling-Guide-v2.pdf

Caruana, R., & Guilizzoni, M. (2025). Modeling of conventional heat pipes with capillary wicks: A review. Energies, 18(9), 2213. https://doi.org/10.3390/en18092213

Chang, C., Fu, B., Ma, X., Yang, X., Lou, T., Xiao, X., & Ji, Y. (2025). Design and thermal analysis of a high-performance flexible heat pipe with all-directional bending. Applied Thermal Engineering, 274, 126783. https://doi.org/10.1016/j.applthermaleng.2025.126783
Egbo, M., Borumand, M., Anuta, U., & Hwang, G. (2026). A review of composite wicks for high heat flux heat pipes and vapor chambers. Applied Thermal Engineering, 285, 129171. https://doi.org/10.1016/j.applthermaleng.2025.129171

DNP. (n.d.). Heat Pipes vs. Vapor Chambers.
https://www.global.dnp/en/biz/column/precision_components/10162048/

Elfa Distrelec. (n.d.). LTO150F47R00JTE3 power resistor, 150 W, 47 Ω. Retrieved May 10, 2026, from Elfa Distrelec.
https://www.elfa.se/sv/effektmotstand-150w-47ohm-vishay-lto150f47r00jte3/p/30213233?trackQuery=effekt%20resistor&pos=5&origPos=14&origPageSize=50&track=true&sid=ozuxZm9xU2&itemList=search

Elfa Distrelec. (n.d.). 7898573 - Kylfläns Svart anodiserad 1K/W 100x125x50mm. Retrieved May 10, 2026.
https://www.elfa.se/sv/kylflaens-svart-anodiserad-1k-100x125x50mm-rs-pro-7898573/p/30404899

Fu, J., & Sundén, B. (2017). Heat Transfer in Aerospace Applications. Elsevier, ISBN: 978-0-12-809760-1. Publisher: Joe Hayton.

Guinan, E., Punch, J., Butler, C., & Egan, V. (2026). Enhancing the resilience of screen mesh wick heat pipes to the degenerative effects of bending-induced deformation. Applied Thermal Engineering, 287, 129328. https://doi.org/10.1016/j.applthermaleng.2025.129328

Guo, H., Ji, X. & Xu, J. (2020). RESEARCH AND DEVELOPMENT OF LOOP HEAT PIPE – A REVIEW.
https://scispace.com/pdf/research-and-development-of-loop-heat-pipe-a-review-3shqq77nps.pdf

Guo, X., Tang, H., Fu, T., & med flera. (2022). *Experimental investigation and multiparameter analysis of variable conductance heat pipes*. *Applied Thermal Engineering, 202*, 117589. https://doi.org/10.1016/j.applthermaleng.2021.117589

Hansen, G., & Næss, E. (2015). Performance of compressed nickel foam wicks for flat vertical heat pipes. Applied Thermal Engineering, 81, 359–367.
https://doi.org/10.1016/j.applthermaleng.2015.02.040

Han, S., Yang, L., Tian, Z., Yuan, X., & Lu, H. (2020). Research on a simplified model of an aluminum vapor chamber in a heat dissipation system. Entropy, 22(1), 35.
https://doi.org/10.3390/e22010035

Huang, S., Wan, Z., Zhang, X., Yang, X., & Tang, Y. (2019). Evaluation of capillary performance of a stainless steel fiber–powder composite wick for stainless steel heat pipe. Applied Thermal Engineering, 148, 1224–1232.
https://doi.org/10.1016/j.applthermaleng.2018.12.014

Jouhara, H., & Meskimmon, R. (2018). An investigation into the use of water as a working fluid in wraparound loop heat pipe heat exchanger for applications in energy efficient HVAC systems. Energy, 156, 597–605. https://doi.org/10.1016/j.energy.2018.05.134

Ku, J. (2015). Introduction to Heat Pipes. NASA/Goddard Space Flight Center. https://tfaws.nasa.gov/wp-content/uploads/TFAWS2015-SC-Heat-Pipes.pdf

Li, Y., Zhou, W., He, J., Yan, Y., Li, B., & Zeng, Z. (2016). Thermal performance of ultra-thin flattened heat pipes with composite wick structure. Applied Thermal Engineering, 101, 1237–1246. https://doi.org/10.1016/j.applthermaleng.2016.03.041

Li, Q., Wang, L., Zhang, D., & Cheng, G. (2025). Vibration-enhanced performance of asymmetric channel flat-plate pulsating heat pipes: Reducing thermal resistance and start-up time under dynamic loads. Applied Thermal Engineering, 281, 128588. https://doi.org/10.1016/j.applthermaleng.2025.128588

Liang, Y., Yan, C., Bai, J., Zhang, M., Zhang, S., Tang, Y., & Yuan, X. (2026). An ultra-thin aluminum flat heat pipe for heat dissipation in aerospace electronic devices. Applied Thermal Engineering, 286, 129384. https://doi.org/10.1016/j.applthermaleng.2025.129384

McClements, D. (2023). Heat Pipe: Definition, Components, Types, Applications, and Factors That Affect Its Performance. Xometry. https://www.xometry.com/resources/3d-printing/what-is-heat-pipe/

Momin, S. H. (2020). Heat pipe technologies and applications. ResearchGate. https://www.researchgate.net/figure/Common-wick-types-of-a-heat-pipe-73_fig12_324811679

Mouser Electronics. (n.d.). ATS-HP-F5L250S35W-027. 250x8.2x2.5mm. Retrieved May 10, 2026. https://www.mouser.se/ProductDetail/Advanced-Thermal-Solutions/ATS-HP-F5L250S35W-027?qs=lc2O%252BfHJPVaZmNP3HQOcfQ%3D%3D

Mouser Electronics. (n.d.). ATS-HP-D6L250S43W-131. 250x6mm. Retrieved May 10, 2026. https://www.mouser.se/ProductDetail/Advanced-Thermal-Solutions/ATS-HP-D6L250S43W-131?qs=w%2Fv1CP2dgqo6w8kG0XbQQA%3D%3D

Mouser Electronics. (n.d.). ATS-HP-F9L250S70W-015. 250x10.5x4.5mm. Retrieved May 10, 2026. https://www.mouser.se/ProductDetail/Advanced-Thermal-Solutions/ATS-HP-F9L250S70W-015?qs=lc2O%252BfHJPVZ%252BWubthl2tIw%3D%3D

Mouser Electronics. (n.d.). ATS-HP-D8L250S62W-149. 250x8mm. Retrieved May 10, 2026. https://www.mouser.se/ProductDetail/Advanced-Thermal-Solutions/ATS-HP-D8L250S62W-149?qs=w%2Fv1CP2dgqqZ5d3uO7boDg%3D%3D

NASA. (1981). *Heat pipe design handbook: Volume I* (NASA-CR-19810065690). NASA. https://ntrs.nasa.gov/api/citations/19810065690/downloads/19810065690.pdf

National Aeronautics and Space Administration. (1981). Heat pipe design handbook (NASA CR-134264). NASA. https://ntrs.nasa.gov/api/citations/19810065690/downloads/19810065690.pdf

Protolabs Network, (n.d.). When to use titanium vs. aluminum in manufacturing. https://www.hubs.com/knowledge-base/when-to-use-titanium-vs-aluminum-in-manufacturing/

Reay, D.A. & Kew, P.A. (2007). *Heat Pipes; Theory, Design and Applications (Fifth Edition)*. Butterworth-Heinemann. https://www.sciencedirect.com/book/monograph/9780750667548/heat-pipes#book-info

Shukla, K. N. (2015). Heat pipe for aerospace applications—An overview. Journal of Electronics Cooling and Thermal Control, 5(1), 1–14. https://doi.org/10.4236/jectc.2015.51001

Sintered Filter. (2023). *Does iron conduct heat? Discover how and why*. Retrieved from https://www.sinteredfilter.net/does-iron-conduct-heat/

Tang, H., Huang, Q., Lu, F., Xu, J., Xie, Y., Sun, Y., Chen, G., & Tang, Y. (2024). *A review of fabrication and performance of heat pipes with grooved wick structure. Applied Thermal Engineering, 255,* 123949. https://doi.org/10.1016/j.applthermaleng.2024.123949

The Engineering Toolbox, (n.d.). Thermal Conductivity of Metals and Alloys: Data Table and Reference. https://www.engineeringtoolbox.com/thermal-conductivity-metals-d_858.html

Tian, X., Zheng, F., Wang, L., Hu, Q., Liang, X., Xu, Y., Qin, J., Zhang, H., & Miao, J. (2025). Heat transfer performance of a novel flat plate heat pipe with sintered aluminum powder wicks. Applied Thermal Engineering, 281, Article 128717. https://doi.org/10.1016/j.applthermaleng.2025.128717

Wakefield Thermal, n.d. Heat pipe selection guide. https://admin.egelectronics.com/wp-content/uploads/2025/03/wfv-heatpipe_designguide_R3_2020.pdf

Wang, G., Chen, Y., Yu, W., Hu, T., Su, H., & Zhu, T. (2025). Heat transfer characteristics of flat-plate micro heat pipes with integrated copper foam for aerospace thermal management. Applied Thermal Engineering, 263, Article 125319. https://doi.org/10.1016/j.applthermaleng.2024.125319

Wang, H., Lin, G., Bai, L., Tao, Y., & Wen, D. (2020). Comparative study of two loop heat pipes using R134a as the working fluid. Applied Thermal Engineering, 164, 114459. https://doi.org/10.1016/j.applthermaleng.2019.114459

Wang, H., Lin, G., Guo, Y., Shen, X., Bai, L., Gong, J., & Su, X. (2025). Experimental study on the operation of a dual compensation chamber loop heat pipe under the effect of vibration. Applied Thermal Engineering, 275, 126878. https://doi.org/10.1016/j.applthermaleng.2025.126878

Wang, Q., & Faghri, A. (2017). A review of loop heat pipes for aircraft anti-icing applications. Applied Thermal Engineering, 125, 1575–1588. https://doi.org/10.1016/j.applthermaleng.2017.07.019

Wang, Z., Xie, G., & Yang, X. (2025). Cellular-engineered titanium heat pipe. Applied Thermal Engineering, 270, 126256.

Xiong, K., Huang, Y., & Wang, S. (2024). Experimental research on the thermal performance of a flat evaporator loop heat pipe with a new composite wick. Applied Thermal Engineering, 246, 122927. https://doi.org/10.1016/j.applthermaleng.2024.122927

Appendix A

Table A1: All possible concept combinations generated using Morpheus.

Concept	Heat pipe	Wick	Working fluid	Material
1	VC	Composite	Ammonia	Al
2	VC	Sintered	Ammonia	Al
3	VC	Composite	Acetone	Al
4	VC	Sintered	Acetone	Al
5	VC	Composite	Methanol	Cu
6	VC	Sintered	Methanol	Cu
7	VC	Composite	Acetone	Cu
8	VC	Sintered	Acetone	Cu
9	VC	Composite	Methanol	SS
10	VC	Sintered	Methanol	SS
11	VC	Composite	Ammonia	SS
12	VC	Sintered	Ammonia	SS
13	VC	Composite	Acetone	SS
14	VC	Sintered	Acetone	SS
15	CHP	Composite	Ammonia	Al
16	CHP	Sintered	Ammonia	Al
17	CHP	Composite	Acetone	Al
18	CHP	Sintered	Acetone	Al
19	CHP	Composite	Methanol	Cu
20	CHP	Sintered	Methanol	Cu
21	CHP	Composite	Acetone	Cu
22	CHP	Sintered	Acetone	Cu
23	CHP	Composite	Methanol	SS
24	CHP	Sintered	Methanol	SS
25	CHP	Composite	Ammonia	SS
26	CHP	Sintered	Ammonia	SS
27	CHP	Composite	Acetone	SS
28	CHP	Sintered	Acetone	SS

Table A2: The possible concepts weighted according to the selected performance criteria.

Concept	Thermal Performance (0.4)	Low temp. performance (0.15)	Orientation independence (0.2)	High temp. performance (0.15)	Mechanical robustness (0.07)	Manufacturability (0.03)	$\sum$	Ranking
1	5	5	3	2	4	2	3.99	17
2	5	5	5	3	3	1	4.44	7
3	4	3	3	4	4	2	3.59	20
4	5	4	5	4	3	1	4.44	7
5	4	2	3	4	4	5	3.53	22
6	5	3	5	5	3	4	4.53	5
7	5	3	3	4	4	4	4.05	13
8	5	4	5	5	3	4	4.68	3
9	2	2	3	5	5	4	2.92	28
10	3	3	5	5	4	3	3.77	18
11	5	5	3	3	4	4	4.20	11
12	5	5	5	4	3	3	4.65	4
13	3	3	3	5	5	4	3.47	24
14	4	4	5	5	4	3	4.32	9
15	4	5	3	3	5	2	3.81	16
16	5	5	5	3	4	1	4.51	6
17	3	4	3	4	5	2	3.41	25
18	4	5	5	5	4	1	4.41	8
19	3	3	3	5	5	4	3.47	10
20	4	4	5	5	4	5	4.38	24
21	4	4	3	5	5	4	4.02	14
22	5	5	5	5	4	5	4.93	1
23	2	3	3	5	5	4	3.07	27
24	3	4	5	5	4	3	3.92	15
25	4	5	3	4	5	4	4.02	14
26	5	5	5	5	4	3	4.87	2
27	2	4	3	5	5	4	3.22	26
28	3	5	5	5	4	3	4.07	12

Table A3: Temperature measurements at 2W in the gravity assisted setup.

Heat Pipe	TC1 – Heat Source (°C)	TC2 – Heat Sink (°C)	ΔT (TC1–TC2)
HP1	30.1	27.9	2.2
HP2	25.5	24.4	1.1
HP3	28.2	25.9	2.3
HP4	28.1	24.3	3.8
HP5	34.6	24.9	9.7
HP6	28.5	24.3	4.2

Table A4: Temperature measurements at 2W in the horizontal setup.

Heat Pipe	**TC1 – Heat Source (°C)**	**TC2 – Heat Sink (°C)**	ΔT **(TC1–TC2)**
HP1	28	26.2	1.8
HP2	26.5	25.7	0.8
HP3	25.4	23.6	1.8
HP4	24.6	23	1.6
HP5	34.3	26.2	8.1
HP6	26.5	25.2	1.3

Table A5: Temperature measurements at 2W in the gravity opposed setup.

Heat Pipe	**TC1 – Heat Source (°C)**	**TC2 – Heat Sink (°C)**	ΔT **(TC1–TC2)**
HP1	29.6	27.9	1.7
HP2	26.9	26	0.9
HP3	26.7	23.9	2.8
HP4	26.7	24.5	2.2
HP5	43	23	20
HP6	36.0	24.4	11.6